forests

MDPI

Article

A Transcriptomic Analysis Sheds Light on the Molecular Regulation of Wood Formation in *Populus trichocarpa* during Drought Stress

Lijuan Dai [1], Bhavana Chaudhari [1], Tianyi Wang [1], Xiang Li [2], Dong Zeng [1], Chunming Li [1,*] and Guanzheng Qu [1,*]

[1] State Key Laboratory of Tree Genetics and Breeding, Northeast Forestry University, Harbin 150040, China; dailijuan0060@163.com (L.D.); vawanach12@gmail.com (B.C.); wangtianyi20001212@163.com (T.W.); zengdong9937@163.com (D.Z.)

[2] School of Agriculture, Ningxia University, Yinchuan 750021, China; lx2016bjfu@163.com

* Correspondence: lichunming@nefu.edu.cn (C.L.); gzqu@nefu.edu.cn (G.Q.); Tel.: +86-18-6463-62087 (G.Q.)

Abstract: Wood is an abundant and essential renewable resource whose production is threatened in some parts of the world by drought. A better understanding of the molecular mechanisms underlying wood formation during drought is critical to maintaining wood production under increasingly adverse environmental conditions. In this study, we investigated wood formation in black cottonwood (*Populus trichocarpa*) during drought stress. The morphological changes during drought stress in *P. trichocarpa* included the wilting and drooping of leaves, stem water loss, and a reduction in whole plant biomass. The water embolism rate indicated that the water transport in stems was blocked under drought conditions. An anatomical analysis of the xylem and cambium revealed that drought stress changed the structure of vessel cells, increased lignin accumulation, and decreased the cambium cell layers. We subsequently identified 12,438 and 9156 differentially expressed genes from stem xylem and cambium tissues under well-watered and drought conditions, respectively. Gene Ontology (GO) and Kyoto Encyclopedia of Genes and Genomes (KEGG) enrichment analyses revealed that these genes were mainly involved in hormone signal transduction and amino sugar and nucleotide sugar metabolism. To further explore the molecular mechanism of wood formation in response to drought, we analyzed the expression patterns of the genes involved in lignin, cellulose, and hemicellulose biosynthesis in xylem and the genes involved in cambial activity in the cambium. To better understand the regulatory networks governing xylem development and cambium activity in response to drought, we analyzed the MYB (138), AP2 (130), bHLH (89), and NAC (81) transcription factor families to shed light on the interactions between the TFs in these families and the genes they regulate. Identifying the key genes that regulate wood formation in *P. trichocarpa* during drought provides a genetic foundation for further research on the molecular regulatory networks and physiology underpinning wood formation during drought stress.

Keywords: drought stress; wood formation; transcriptomic sequencing; xylem; cambium; *Populus trichocarpa*

Citation: Dai, L.; Chaudhari, B.; Wang, T.; Li, X.; Zeng, D.; Li, C.; Qu, G. A Transcriptomic Analysis Sheds Light on the Molecular Regulation of Wood Formation in *Populus trichocarpa* during Drought Stress. *Forests* **2024**, *15*, 873. https://doi.org/10.3390/f15050873

Academic Editor: Stéphane Maury

Received: 24 April 2024
Revised: 9 May 2024
Accepted: 15 May 2024
Published: 17 May 2024

1. Introduction

Wood formation is a complex developmental process comprising sequential rounds of cell proliferation/differentiation (CPD), cell expansion (CE), secondary cell wall (SCW) thickening, and programmed cell death (PCD) [1]. In the stem cambium, CPD is regulated by structural genes [2], functional proteins [3], and plant hormones [4]. Auxin stimulates cambial growth and mediates multiple stages of xylem development. Regulated auxin transport and auxin-responsive genes in wood-forming tissues regulate cambial activity and xylem differentiation during wood formation [5–7]. Brassinosteroid activates WALLS ARE THIN1 (WAT1), a critical regulator of local auxin homeostasis and signaling outputs

in the vascular cambium that facilitates wood formation in *Solanum lycopersicum* [8]. These studies highlight the importance of plant hormones in cell proliferation and differentiation in vascular tissues during wood formation.

Populus trichocarpa, also known as black cottonwood, is a pivotal species in the wood industry due to its rapid growth, high biomass yield, and suitability for bioenergy and pulp production. In the stem xylem of *P. trichocarpa*, CE, SCW thickening, and PCD are regulated by metabolites, biosynthesis of secondary cell wall components, and complex molecular networks. Wood formation requires secondary xylem cells in the vascular cambium to differentiate into fibers, vessel elements, and ray cells concurrent with the biosynthesis of the major cell wall components: cellulose, hemicellulose, and lignin [9]. Cellulose and hemicellulose are major components of the primary cell wall, which play an important role in CE. The metabolic pathway regulating UDP-sugar accumulation, a substrate used for the synthesis of these polysaccharides, also plays an important role in cell wall biosynthesis [10]. Proteins associated with cellulose and hemicellulose, as well as xylem-specific transcription factors regulating SCW biosynthesis, have been identified in *P. trichocarpa*. These include 14 proteins that have been accurately and precisely quantified during tree development and environmental stress, which are essential for uncovering the changes in cellulose biosynthesis [11]. Whereas cellulose and hemicellulose are necessary for SCW biosynthesis, lignin is a complex polymer that is required for SCW thickening [12]. The main building blocks of lignin are the monolignols guaiacyl (G), syringyl (S), and p-hydroxyphenyl (H). Interestingly, the ratio of these monolignols in the lignin polymer contributes to varying degrees of abiotic stress tolerance in the poplar [13]. The identification of genes encoding specific monolignol biosynthetic enzymes in *P. trichocarpa* and their functional characterization has revealed that the precise ratio of monolignols in lignin is determined by the tightly regulated activity of these enzymes [14–16].

Cambial activity and xylem development during stem growth under drought conditions are known to negatively affect wood formation [17–19]. Specifically, drought stress can cause morphological, transcriptional, metabolic, and hormonal changes [20,21]. Drought directly promotes the ability of the transcription factors PtoMYB170 and PtrbHLH186 to bind AC- and G-box elements in the promoters of lignin biosynthetic genes in woody plants [22]. Transgenic *Morus alba*, expressing the gene encoding cinnamyl-alcohol dehydrogenase (CAD), which catalyzes the final step of monolignol biosynthesis, revealed that the MaCAD family members are responsible for the formation of various monolignols in lignin biosynthesis under drought stress [23]. Overexpression of the *Pennisetum purpureum PpCCoAOMT* gene promotes lignin accumulation, which is associated with drought tolerance and reduced accumulation of reactive oxygen species [24]. The phytohormones auxin [25,26], cytokinin [27], gibberellin [28,29], brassinosteroids [30], ethylene [31], and abscisic acid [32,33] form a complex regulatory network that controls both vascular cell development during wood formation and plant responses to drought [34].

A comprehensive analysis of the impact of drought on gene regulation during wood formation would help answer some important lingering questions. For instance, it is still unknown how cambial activity is affected in the stem and how PD, CE, SCW thickening, and PCD are regulated during wood formation in the stem xylem and cambium under drought stress. In this study, we conducted a transcriptomic analysis of *P. trichocarpa's* stem xylem and cambium during wood formation under drought stress to better understand the role of hormone signaling, sugar metabolism, and transcription factors in regulating wood formation under this adverse condition. This study is expected to elucidate the molecular regulatory mechanisms associated with drought response, aiding in the identification of key genes or regulatory pathways, thereby enhancing the drought tolerance of crop plants. This will make agricultural production systems more resilient to drought, thus better adapting to the challenges of climate change.

2. Materials and Methods

2.1. Plant Materials and Drought Treatment

P. trichocarpa plants were raised in 15 cm pots (one plant per pot) in a greenhouse under long-day conditions (16 h light/8 h dark) at 23–25 °C as described previously [35]. Four-month-old plants of similar size and vigor were selected for the drought treatments. The plants were well-watered up until the time of treatment, with the control plants continuing to be watered while water was withheld from the drought-treated plants. The soil volumetric water content (VWC) was measured every day using a soil moisture meter (TDR 250; Spectrum Technologies, Aurora, CO, USA) as described previously [36]. Measurements of the VWC were taken at the beginning, middle, and end of each day for 5–7 days during the drought treatment to determine the final soil VWC (the soil VWC of the control: 65%; the soil VWC of drought: 19%). Tissue for the RNA-seq was collected from the stem cambium and included cambium zone cells and slight secondary phloem cells. Cambium zone cells under control (WC) or drought (DC) conditions were kept separate from the stem xylem (differentiating xylem) under control (WX) or drought (DX) conditions. The tissue was collected between the seventh and basal internodes and flash-frozen directly in liquid nitrogen, where it was kept until all samples had been harvested.

2.2. Quantification of Biomass and the Water Embolism Rate

The plants were cut at the base of the stem, and the fresh weight of all leaves and the whole stem for each plant were measured after the control and drought treatments to determine the effects of drought on the biomass. The XYL'EM-Plus xylem hydraulic conductivity and embolism measurement system was used to determine the water embolism rate. This was conducted by using the reference 'water pressure' method to first measure the hydraulic conductivity (HC1) of the internodes that were 1 cm in length under low pressure. The air within the xylem embolism catheter was then removed using high-pressure continuous perfusion to saturate the water. The hydraulic conductivity (HC2) under low pressure was then measured again, and the water embolism rate was calculated using the formula below [37].

$$Water\ embolism\ rate\ (\%) = \frac{HC2 - HC1}{HC2} \times 100\%$$

2.3. Analysis of Wood Anatomy

The stem internodes of wild-type *P. trichocarpa* were cut into 1 mm fragments, and paraffin sectioning was performed as described previously [36]. The target stem segments were cut into sections that were roughly 10 µm thick using a rotary microtome (RM2245; Leica, Weztlar, Germany). Sections were stained with toluidine blue to observe the cambium zone and stained with phloroglucinol-HCl to observe lignin. Micrographs of the stem cross-sections were taken using a Scanner M8 (FM34F056; PreciPoint Lang Drake, TX, USA) and VIEWPOINT (v1.0.0.0) setup software.

2.4. RNA Extraction and Sequencing

Total RNA from the stem xylem or cambium tissue of *P. trichocarpa* wild-type plants under well-watered or drought treatments was extracted using a Qiagen RNeasy Plant Mini Kit. The DNA was digested for 15 min using an RNase-Free DNase Set (QIAGEN, Hilden, Germany) to remove contamination from the genomic DNA. The quality of the purified RNA was determined using a Bioanalyzer 2100 (Agilent, Santa Clara, CA, USA). Ribosomal RNA (rRNA) was removed from the total RNA by hybridizing the rRNA to a DNA probe and digesting the DNA/RNA hybrid strands with RNaseH. The DNA probe was then degraded with a DNase I treatment. The mRNA was then used as a template to synthesize first-strand cDNA. This was followed by double-stranded cDNA synthesis using a two-strand synthesis reaction. The quality and quantity of the constructed libraries were assessed using an Agilent 2100 Bioanalyzer and an ABI StepOnePlus Real-Time PCR

System. A total of 12 libraries were sequenced using an Illumina HiSeq platform. After removing the library index sequences from each read, the clean reads were mapped to the *P. trichocarpa* genome v.3.0 (https://phytozome-next.jgi.doe.gov/info/Ptrichocarpa_v3_0, accessed on 14 May 2024) using Bowtie2 [38].

2.5. Identifying Differentially Expressed Genes

Differentially expressed genes (DEGs) were identified between the stem cambium and xylem tissues under multiple conditions, with three biological replicates used per treatment condition [39]. A negative binomial distribution was used in DESeq to determine if the genes were differentially expressed between treatments. Furthermore, *p*-values were adjusted using Benjamini and Hochberg's false discovery rate (FDR) with a *p*-adjust value of <0.05 and a |log2Fold Change (FC)| of ≥1 used as a threshold to classify genes as differentially expressed. To understand the biological function of the DEGs, Gene Ontology (GO) and Kyoto Encyclopedia of Genes and Genomes (KEGG) enrichment analyses were performed using the GOseq R package 2.10 and KOBAS 2.0 software, respectively. The transcription factors (TFs) were predicted using PlantTFDB (http://planttfdb.gao-lab.org/). The interactions were analyzed using STRING (https://cn.string-db.org/) (version 11.5), and interaction networks were constructed using Cytoscape (3.7.2).

2.6. Quantitative Reverse-Transcription PCR (qRT-PCR)

A total of 200 ng of RNA was used for synthesizing cDNA with the PrimeScript RT kit (TaKaRa, Kusatsu, Japan). qRT-PCR was performed in triplicate on an Agilent M×3000P Real-Time PCR System using the TB Green Premix Ex Taq II (Tli RNaseH Plus) kit (TaKaRa). A single 20 µL reaction mixture comprised 10 µL of 2× TB Green Premix Ex Taq, 2 µL of cDNA template, 6 µL of ddH_2O, 0.8 µL of upstream and downstream primers, and 0.4 µL of ROX reference dye. The PCR reaction conditions were as follows: 95 °C for 10 min, 40 cycles at 95 °C for 30 s, and 60 °C for 1 min, followed by 95 °C for 1 min, 55 °C for 30 s, and 95 °C for 30 s. The relative expression levels of all the DEGs were calculated using the $2^{-\Delta\Delta Ct}$ method [40]. The primers used for qRT-PCR can be found in Supplementary Table S1.

2.7. Statistical and Visualization Analysis

Raw data were analyzed using Excel 2016 (Microsoft Corp., Albuquerque, NM, USA). Analysis of variance (ANOVA) was performed using SPSS 25.0 statistical software (IBM Crop, Armonk, NY, USA) with the S–N–K significant difference test at $p < 0.05$. Heatmaps and the UpSet diagram were created with TBtools (v1.1043).

3. Results

3.1. Morphological and Anatomical Analyses of P. trichocarpa under Drought Stress

We subjected the wild-type plants to control and drought conditions (as described in the Materials and Methods section) to better understand the response of *P. trichocarpa* to drought stress. At 3 months of age, the drought treatment was initiated with a starting soil VWC of 65.8% (Figure 1a). The soil VWC of the control group was maintained at 65% through the duration of the experiment, whereas the soil VWC of the drought-treated plants declined from 65% to 19% (Figure 1b). At the Drought-1 stage (35.4% soil VWC), leaves 2–5 displayed a slight wilting phenotype. Signs of severe wilting were evident in just the first leaf at the Drought-2 stage (19% soil VWC), and the fresh weight of the stems and leaves was significantly lower than at Drought-1 (Figure 1c,d). The water embolism rate of the stems, a reference index for evaluating the severity of drought stress in plants, was much higher in the plants subjected to drought than in the control plants (Figure 1e).

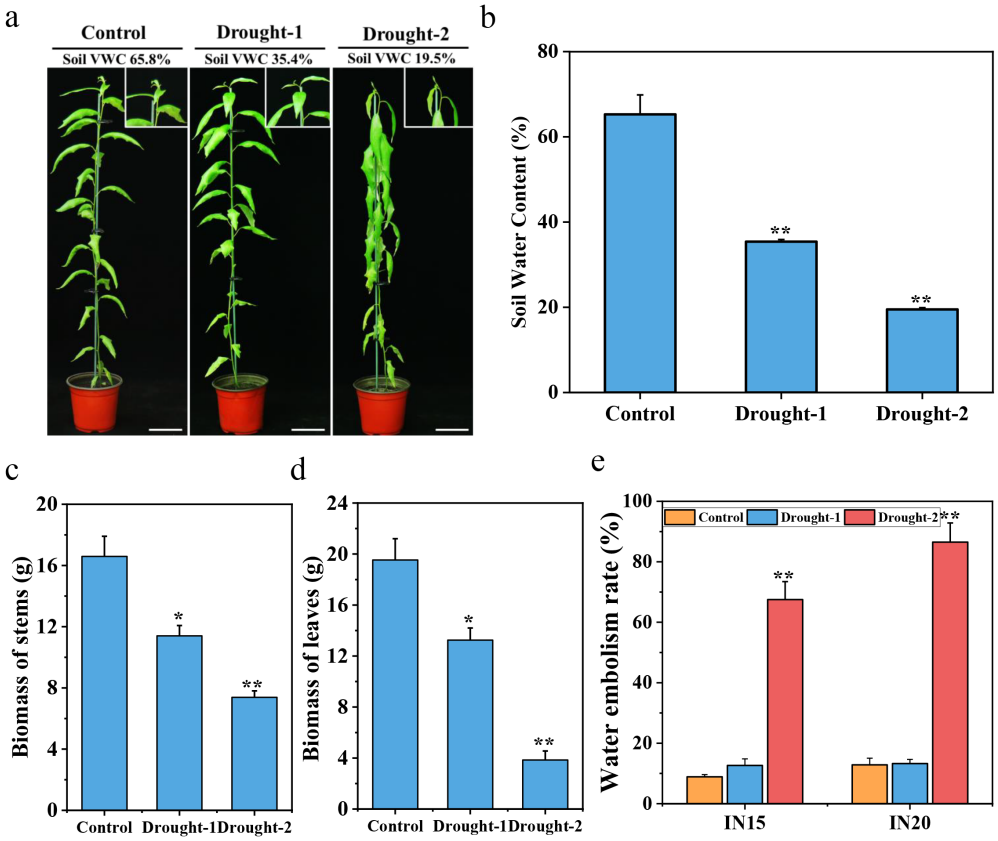

Figure 1. Morphological and anatomical analyses of plants under control and drought conditions. (**a**) Images of whole *P. trichocarpa* plants taken under control, Drought-1, and Drought-2 conditions. The scale bar is equal to 8.5 cm. (**b**) Quantification of soil VWC under control, Drought-1, and Drought-2 conditions. (**c**) Quantification of stem biomass and (**d**) leaf biomass under control and drought conditions. (**e**) Quantification of the water embolism rate between the 15th and 20th internodes under control and drought conditions. Error bars indicate the mean ± SE (n = 3) from three independent experiments. A two-tailed Student's t-test was used to determine statistical significance. * $p < 0.05$ and ** $p < 0.01$.

The xylem plays an essential role in hydraulic conduction during wood formation. To assess the impact of drought stress on the xylem morphology, we performed scanning electron microscopy on the control and drought-treated plant stems (Figure 2a). Our imaging analysis revealed that *P. trichocarpa*, subjected to drought, had a smaller vascular luminal area and a higher vessel density compared with the control plants (Figure 2c–e). Additionally, lignin-specific histochemical staining revealed that drought stress resulted in increased lignin accumulation (Figure 2b). Toluidine blue staining of the cambium zone revealed that drought stress resulted in fewer cambium cell layers (Figure 2b). These findings indicate that drought alters the anatomical structure of the xylem and cambium cells in the stem of *P. trichocarpa*.

3.2. Functional Classification of DEGs Using GO and KEGG Enrichment

We assessed the transcriptional profiles of the stem xylem and cambium tissues under drought stress to explore the impact of drought on the wood formation in *P. trichocarpa*. A range of 26–38 million reads were generated from the samples, which yielded an average of ~24 million clean reads that were used for subsequent bioinformatic analyses after filtering and sequencing error checks. The average Q20 and total mapped reads were 98.09% and 89.6%, respectively, indicating the reads were of good overall quality (Supplementary Table S2). We identified 12,438 DEGs (4782 upregulated and 7656 downregulated) between the cambium cells under control (WC) versus drought (DC) conditions. The number of

DEGs between the xylem cells under control (WX) versus drought (DX) conditions was 9156 (5008 upregulated and 4148 downregulated) (Figure 3a). Among these DEGs, 6366 and 3084 were specific to the stem cambium and xylem, respectively, whereas 6072 were common in both the cambium and xylem (Figure 3b).

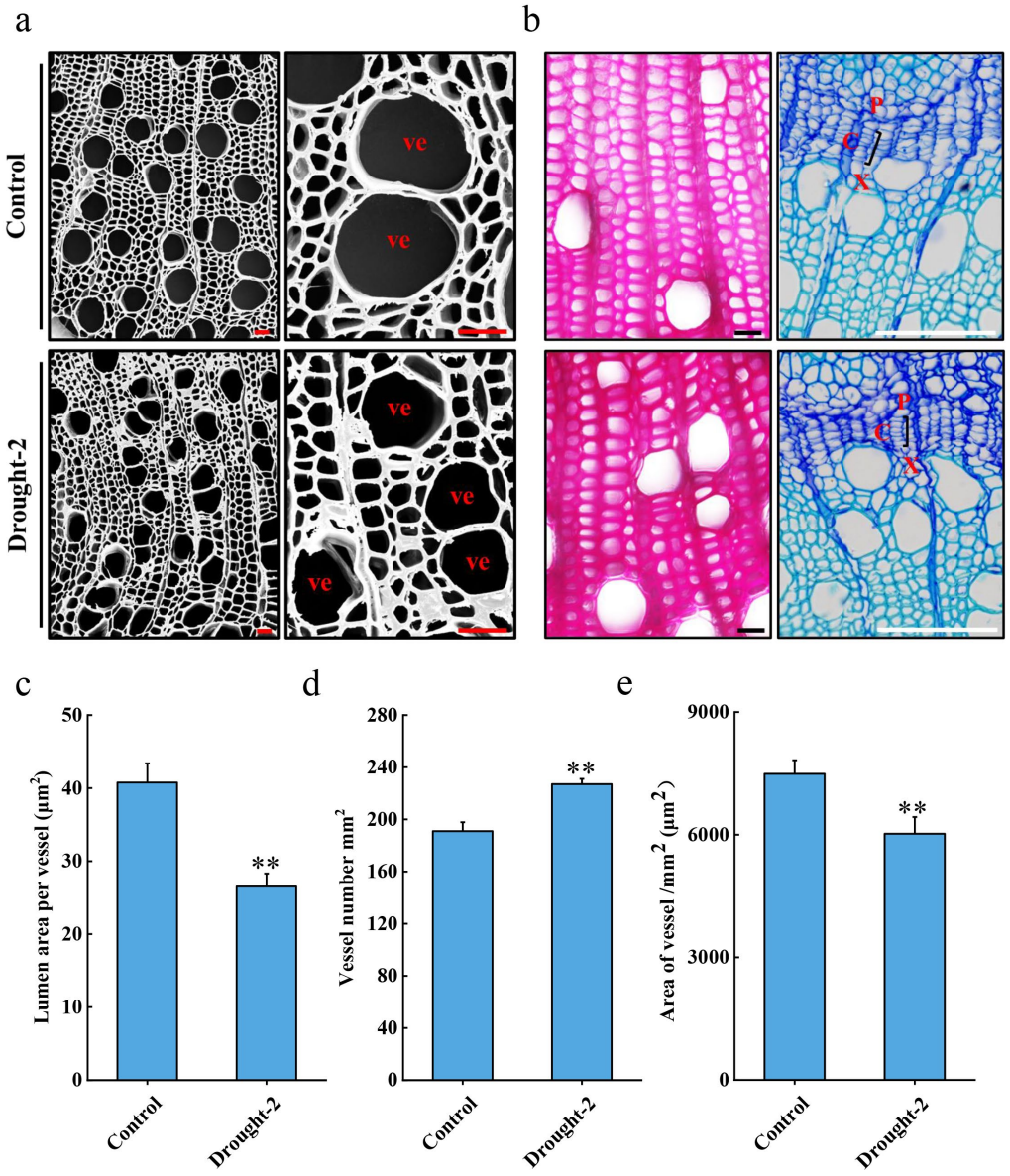

Figure 2. Analyses of xylem and cambium morphologies and lignin deposition under drought stress. (**a**) Stem cross-sections taken from the 15th internode of plants under control and Drought-2 conditions were observed with a scanning electron microscope (SEM). Red scale bars are equal to 100 μm, vessel cell (ve). (**b**) Lignin-specific histochemical and toluidine blue staining of stem cross-sections taken from the 15th internode of plants under control and Drought-2 conditions. The black scale bars are equal to 20 μm, and the white scale bars are equal to 100 μm, xylem zone (X), cambium zone (C), and phloem zone (P). (**c**) Quantification of lumen area per vessel, (**d**) vessel number, and (**e**) area of the vessel. Error bars indicate the mean ± SE (n = 3) from six sections per three independent experiments. A two-tailed Student's t-test was used to assess statistical significance; ** $p < 0.01$.

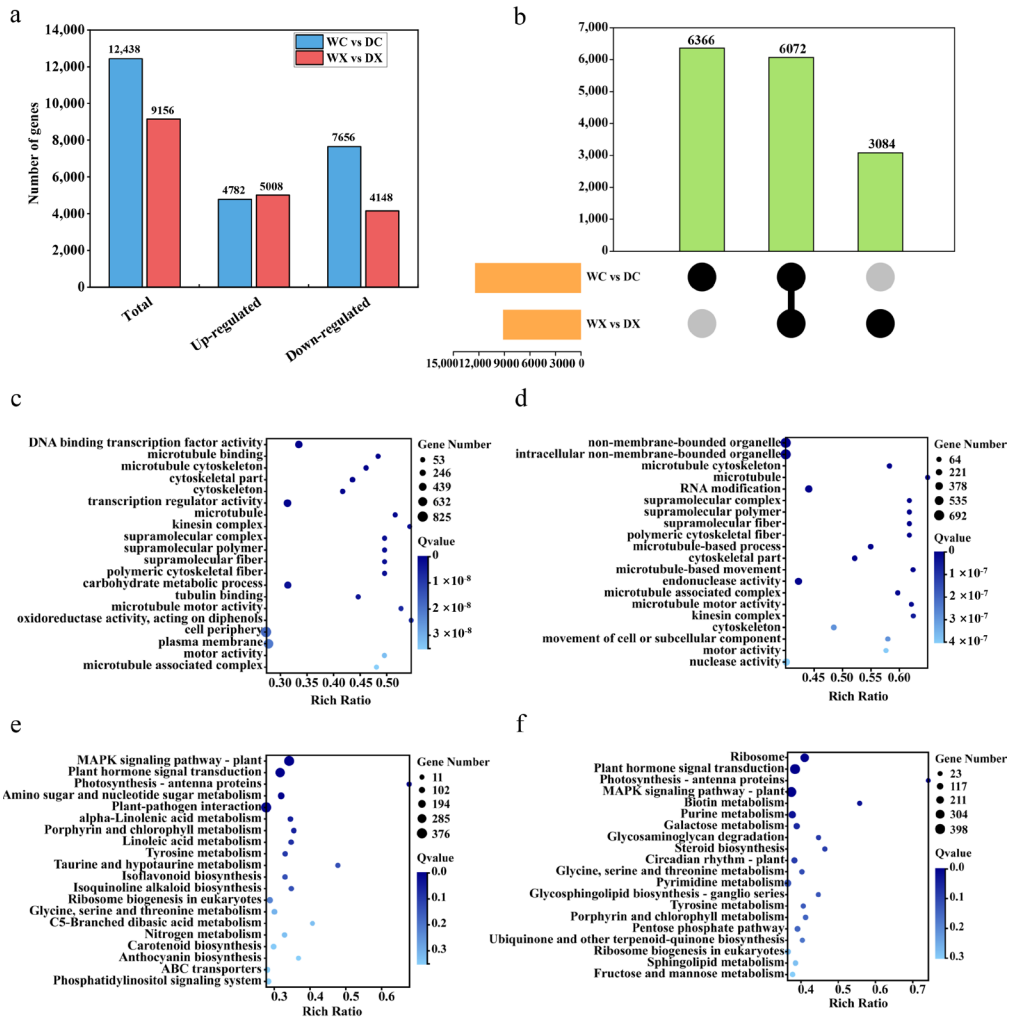

Figure 3. Identification and functional enrichment of DEGs (differentially expressed genes) in WX (xylem under control) versus DX (xylem under drought) and WC (cambium under control) versus DC (cambium under drought). (**a**) Statistical analyses of upregulated and downregulated DEGs under different treatment conditions. (**b**) UpSet diagram of DEGs under different treatment conditions. (**c**) GO enrichment analysis for DEGs between WX and DX. (**d**) GO enrichment analysis for DEGs between WC and DC. (**e**) KEGG enrichment analysis for DEGs between WX and DX. (**f**) KEGG enrichment analysis for DEGs between WC and DC. The color scale represents $\log_2$ fold-change values with light blue to dark blue, indicating expression values from low to high, respectively. The area of the circle represents the number of genes annotated with the given term.

We next performed a GO annotation enrichment analysis on the DEGs to better assess their biological function. Many of the DEGs could be grouped into three GO categories as follows: biological process (BP), molecular function (MF), and cellular component (CC). Of the DEGs in the stem xylem tissue, twelve were annotated as CP, one as BP, and seven as MF (Figure 3c, Supplementary Table S3). Of the DEGs in the stem cambium tissue, twelve2 were annotated as CP, four as BP, and four as MF (Figure 3d, Supplementary Table S4). A KEGG pathway enrichment analysis revealed that most of the DEGs were involved in amino sugar and nucleotide sugar metabolism (ko00520) and the plant hormone signal transduction pathway (ko04075) in both tissues (Figure 3e,f, Supplementary Tables S5 and S6).

3.3. Analysis of Plant Hormone Signal Transduction Pathways

Plant hormones play an important role in signaling during the drought response and regulate the wood formation in stem cambium tissue [41]. We identified 77 DEGs from the stem xylem and cambium of *P. trichocarpa* that are associated with the signal

transduction pathways for eight plant hormones (Figure 4, Supplementary Table S7). Three genes encoding AUX/IAA were significantly downregulated in the stem cambium tissues in response to drought, whereas three genes encoding ABF in the abscisic acid pathway were significantly upregulated under the drought conditions. In the jasmonic acid and ethylene pathways, eight genes encoding JAZ, four genes encoding ERF1/2, and four genes encoding EIN3 were significantly upregulated in the stem xylem tissues in response to drought. A few genes in the salicylic acid and brassinosteroid pathways were slightly downregulated in the stem xylem tissues. In general, the expression patterns of the DEGs involved in the plant signal transduction pathways in the stem xylem and cambium tissues indicated that drought inhibited cambium activity and accelerated xylem differentiation by suppressing the expression of the auxin and cytokinin transport channels. This likely inhibits stem growth and accelerates lignification. Moreover, our results provide insight into the complex relationship between plant hormones and cambium activity and xylem development [42].

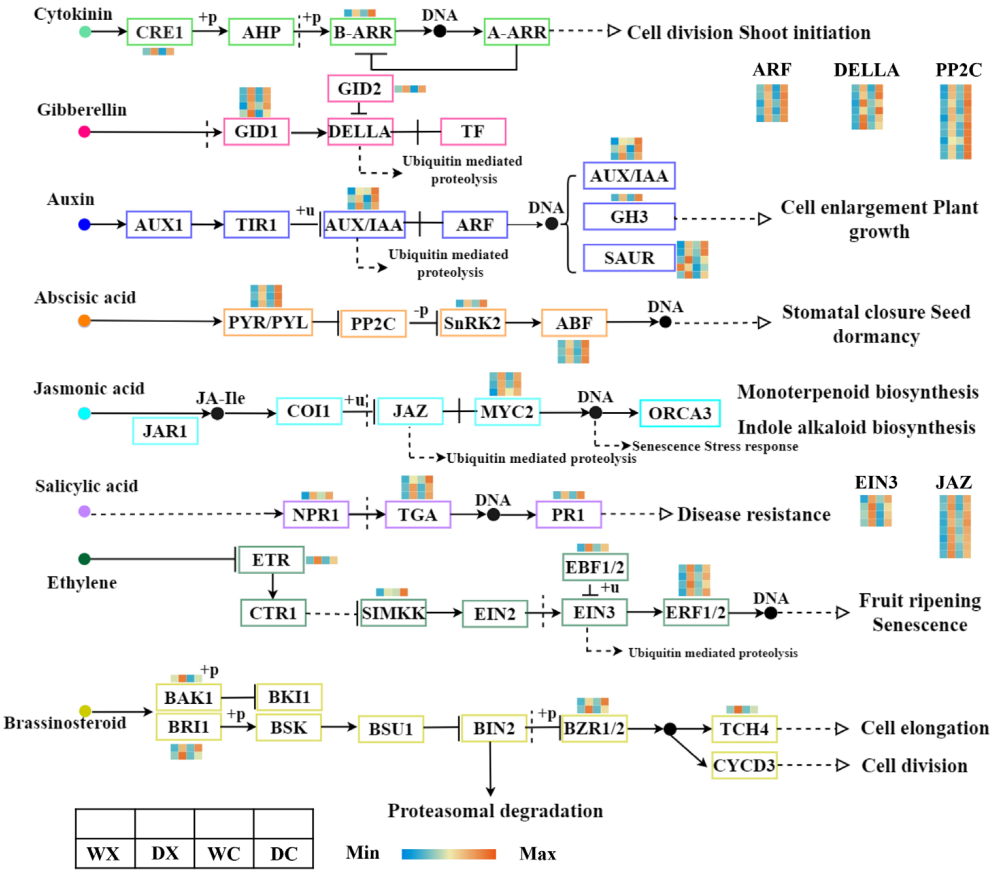

Figure 4. Analyses of DEGs related to the plant hormone signal transduction pathway. Abbreviations: xylem under control (WX); xylem under drought (DX); cambium under control (WC); cambium under drought (DC); cytokinin receptor (CRE1); histidine-containing phosphotransfer protein (AHP); two-component response regulator ARR-B family (B-ARR); two-component response regulator ARR-A family (A-ARR); gibberellin receptor (GID1); F-box protein (GID2); DELLA protein (DELLA); auxin influx carrier (AUX1); transport inhibitor response 1 (TIR1); auxin-responsive protein IAA (AUX/IAA); auxin response factor (ARF); auxin-responsive GH3 gene family (GH3); SAUR family protein (SAUR); abscisic acid receptor PYR/PYL family (PYR/PYL); protein phosphatase 2C (PP2C); serine/threonine-protein kinase SRK2 (SnRK2); ABA-responsive element-binding factor

(ABF); jasmonic acid-amino synthetase (JAR1); coronatine-insensitive protein 1 (COI1); jasmonate ZIM domain-containing protein (JAZ); transcription factor MYC2 (MYC2);regulatory protein NPR1 (NPR1); transcription factor TGA (TGA); pathogenesis-related protein 1 (PR1); ethylene receptor (ETR); mitogen-activated protein kinase kinase 4/5 (SIMKK); EIN3-binding F-box protein (EBF1/2); ethylene-insensitive protein 3 (EIN3); ethylene-responsive transcription factor 1 (ERF1); brassinosteroid insensitive 1-associated receptor kinase 1 (BAK1); protein brassinosteroid insensitive 1 (BRI1); BR-signaling kinase (BSK); brassinosteroid resistant 1/2 (BZR1/2); xyloglucan: xyloglucosyl transferase TCH4 (TCH4); cyclin D3 (CYCD3). The color scale represents the log2 fold-change in gene expression, with the lowest expression represented by blue to the highest expression in red.

3.4. Analyses of the Amino Sugar and Nucleotide Sugar Metabolism Pathways

Primary cell wall biosynthesis and secondary cell wall thickening occur throughout the process of wood formation [43]. We decided to focus our analysis on the pentose and glucuronate interconversion pathways, the glycolysis and gluconeogenesis pathways, and the galactose metabolism pathway. These pathways provide the UDP-sugar metabolism that is essential for cell wall formation (Figure 5). A total of 33 genes were identified, including 14 related coding proteins (Supplementary Table S8). The genes encoding abfA (1 gene), UXE (4 genes), and galE (2 genes) were significantly upregulated in the stem xylem and cambium tissues in response to drought, whereas two genes encoding 1,4-beta-D-xylan synthase (E2.4.2.24) were significantly downregulated in the stem cambium tissues in response to drought. The genes encoding XYL4 (6 genes), USP (1 gene), GALAK (1 gene), GAUT (2 genes), and UXS1 (2 genes) were significantly downregulated in the stem xylem tissues in response to drought. Embolism formation, as a consequence of drought, led to an altered metabolic profile in the cambium and xylem. This led to the upregulation of the genes involved in disaccharide metabolism and the downregulation of the genes involved in monosaccharide metabolism. These changes in carbohydrate metabolism promoted starch degeneration and intracellular and extracellular osmotic pressure increases, which provided energy for the stem to resist drought stress [44].

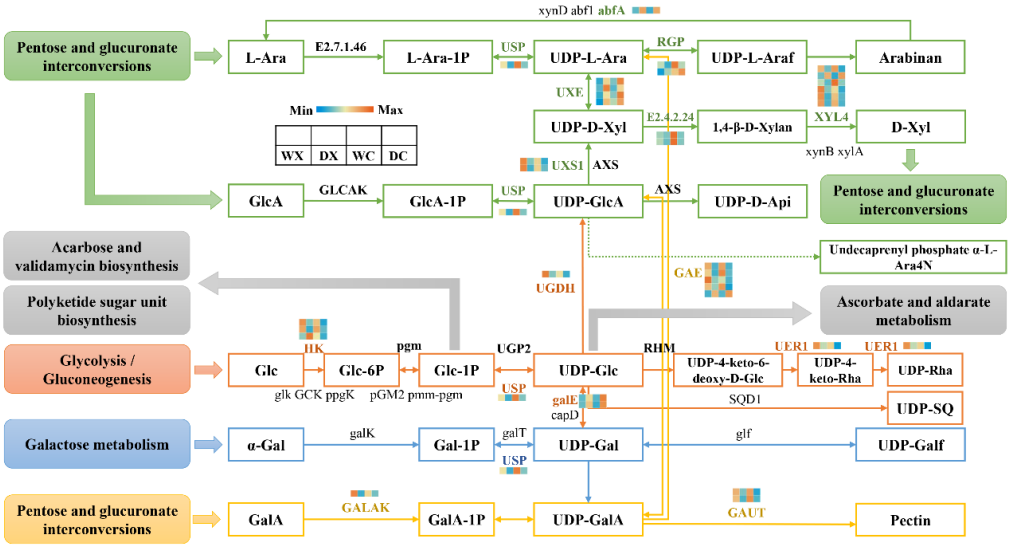

Figure 5. Analyses of DEGs related to the amino sugar and nucleotide sugar metabolism pathways. Abbreviations: xylem under control (WX); xylem under drought (DX); cambium under control (WC); cambium under drought (DC); L-Arabinose (L-Ara); beta-L-Arabinose 1-phosphate (L-Ara-1P); UDP-L-arabinose (UDP-L-Ara); UDP-L-arabinofuranose (UDP-L-Araf); UDP-D-xylose (UDP-D-Xyl); 1,4-beta-D-Xylan (1,4-β-D-Xylan); D-Xylose (D-Xyl); D-Glucuronate (GlcA); D-Glucuronate 1-phosphate

(GlcA-1P); UDP-glucuronate (UDP-GlcA); UDP-apiose (UDP-D-Api); alpha-D-Glucose (Glc); D-Glucose 1-phosphate (Glc-1P); alpha-D-Glucose 6-phosphate (Glc-6P); UDP-glucose (UDP-Glc); UDP-4-dehydro-6-deoxy-D-glucose (UDP-4-keto-6-deoxy-D-Glc); UDP-4-keto-rhamnose (UDP-4-keto-Rha); UDP-L-rhamnose (UDP-Rha); UDP-6-sulfoquinovose (UDP-SQ); UDP-alpha-D-galactofuranose (UDP-Galf); alpha-D-Galactose (α-Gal); alpha-D-Galactose 1-phosphate (Gal-1P); UDP-alpha-D-galactose (UDP-Gal); D-Galacturonate (GalA); 1-Phospho-alpha-D-galacturonate (GalA-1P); UDP-D-galacturonate (UDP-GalA); L-arabinokinase (E2.7.1.46); 1,4-beta-D-xylan synthase (E2.4.2.24); hexokinase (HK); alpha-L-arabinofuranosidase (abfA); UDP-glucose 4-epimerase (galE); phosphoglucomutase (pgm); UDP-glucuronate decarboxylase (UXS1); UDP-glucuronate 4-epimerase (GAE); UDP-sugar pyrophosphorylase (USP); UDP-arabinose 4-epimerase (UXE); UDP-apiose/xylose synthase (AXS); UDP-glucose 4,6-dehydratase (RHM); 3,5-epimerase/4-reductase (UER1); UDP-arabinopyranose mutase (RGP); xylan 1,4-beta-xylosidase (XYL4); glucuronokinase (GLCAK); UTP-glucose-1-phosphate uridylyltransferase (UGP2); alpha-1,4-galacturonosyltransferase (GAUT); UDPglucose 6-dehydrogenase (UGDH); galacturonokinase (GALAK). The color scale represents the $\log_2$ fold-change in gene expression, with the lowest expression represented by blue to the highest expression in red.

3.5. Analysis of Xylem Development under Drought Stress

Lignin, cellulose, and hemicellulose are important components of the primary and secondary cell walls that play key roles in the development of xylem cells [45]. We performed a cluster analysis of the genes related to the monolignol (Figure 6a), cellulose (Figure 6b), and hemicellulose (Figure 6c) biosynthesis pathways to better understand how the lignin, cellulose, and hemicellulose metabolisms were affected during drought. Notably, drought stress affected the expression of the genes related to the monolignol biosynthesis pathway in *P. trichocarpa*. This was especially apparent in the stem xylem tissue (Supplementary Table S9), where one *PAL* gene was upregulated in response to drought, whereas one *COMT* gene, one *C3H* gene, and two *4CL* genes were significantly downregulated. Interestingly, most genes related to monolignol biosynthesis were downregulated in the xylem under drought stress. Genes related to cellulose biosynthesis were also largely downregulated under drought stress. Specifically, *PtrCesA15*, *PtrCesA2*, and *PtrCesA14* were primarily expressed in the cambium, and *PtrCesA8*, *PtrCesA4*, *PtrCesA18*, *PtrCesA7*, and *PtrCesA17* were primarily expressed in the xylem. Most genes related to hemicellulose biosynthesis were significantly downregulated in the xylem under drought stress, whereas *PtrPARVUS-L-1*, which had higher expression in the cambium, was upregulated. To verify the accuracy of our transcriptomic data, we used qRT-PCR to validate the expression pattern of the 16 genes specifically expressed in the xylem of *P. trichocarpa* (Supplementary Figure S1). The qRT-PCR results showed that the key genes involved in the xylem development were significantly downregulated in the xylem in response to drought, consistent with the RNA-seq analysis.

3.6. Analysis of Cambial Activity under Drought Stress

In poplar, LBD3, WOX4, HB4, and HB7 regulate the cambial activity by regulating plant hormones and other factors that affect wood formation directly or indirectly [26,46–48]. We analyzed the expression patterns of 19 of these genes in the cambium using our transcriptomic data (Table 1). Most of these genes were significantly downregulated in response to drought, such as *PtrHB4* and *PtrHB7*, whereas only four genes were significantly upregulated. Interestingly, *LBD3a* and *LBD3b* expression was inversely related in the cambium (Supplementary Table S10). We used homologous proteins in Arabidopsis to predict the protein interactions by STRING, and interactions between some of these proteins were found, such as WOX4, LBD4, and PXY. We also used qRT-PCR to validate the expression of 12 DEGs related to cambial activity in the cambial tissue of *P. trichocarpa* randomly (Supplementary Figure S2). The expression of these DEGs in the cambium was consistent with the results from the RNA-seq analysis and confirmed that the expression of these genes is inhibited in response to drought. Most DEGs with functions related to the cambium

were downregulated in response to drought in the cambium. The expression of these DEGs provides new insights into how the cambium responds to drought.

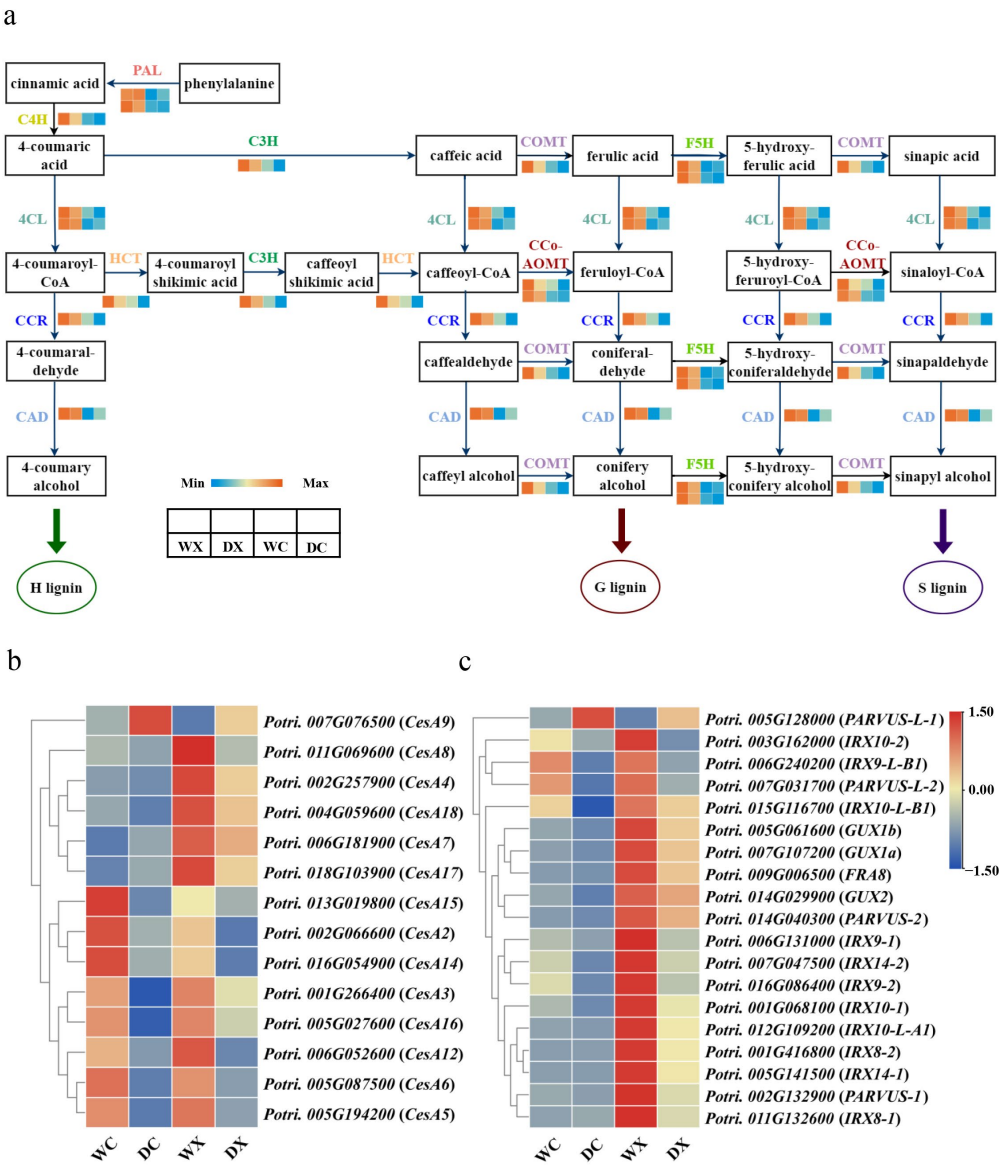

Figure 6. Analyses of DEGs related to the monolignol, cellulose, and hemicellulose biosynthesis pathways. (**a**) DEGs related to the monolignol biosynthesis pathway. (**b**) Heatmaps of DEGs related to cellulose, and (**c**) hemicellulose biosynthesis. Abbreviations: xylem under control (WX); xylem under drought (DX); cambium under control (WC); cambium under drought (DC); phenylalanine ammonia-lyase (PAL); 4-coumarate-CoA ligase (4CL); ferulate-5-hydroxylase (F5H); cinnamoyl-CoA reductase (CCR); shikimate O-hydroxycinnamoyltransferase (HCT); caffeic acid 3-O-methyltransferase/acetylserotonin O-methyltransferase (COMT); cinnamyl-alcohol dehydrogenase (CAD); caffeoyl-CoA O-methyltransferase (CCoAOMT); trans-cinnamate 4-monooxygenase (C4H); 5-O-(4-coumaroyl)-D-quinate 3′-monooxygenase (C3H). The color scale represents the $\log_2$ fold-change in gene expression, with the lowest expression represented by blue to the highest expression in red.

Table 1. Functional analyses from the literature of homologs to the DEGs identified in this study related to cambium activity in the cambium.

Gene ID	Gene Name	Species	Method Used for Characterization	Plant Age	Function	References
Potri. 014G039900	*PagDA1a*	*P. alba* × *P. glandulosa*	*PagDA1a/1b* overexpressing lines	3-month	The PagDA1-PagWOX4 regulatory complex is involved in cambial activity during wood formation	[47]
			PagDA1a/1b/1a-b knockout mutants	3-month		
Potri. 014G025300	*PagWOX4a*		*PagWOX4a/b*-RNAi lines in WT	3-month		
Potri. 002G124100	*PagWOX4b*		*PagWOX4a/b*-RNAi lines in *da1*mutants	3-month		
Potri. 012G100200	*VCM1*	*P. deltoides* × *P. euramericana* 'Nanlin895'	*PtrVCM1*-overexpressing lines	3-mouth	Regulation of vascular cambium proliferation activity and xylem tissue increment in Populus	[5]
Potri. 015G098400	*VCM2*		*PtrVCM1-2*-RNAi lines	3-month		
Potri. 007G066700 Potri. 001G081400	*AtLBD4*	*A. thaliana*	*tmo6 wox14* double mutants and *tmo6 wox14 lbd4* triple mutants	5-week	Critical for controlling vascular proliferation and shape as feed-forward loop transcription factors	[49]
Potri. 001G049700	*AtCLE44*		*cle41 cle42 cle43 cle44* quadruple mutants	5-week	PXY/TDIF activates the expression of all genes within the feed-forward loop	
Potri. 003G107600 Potri. 001G126100	*AtWOX4* (*AtPXY*)		*pxy* mutants and *wox4 wox14* double mutants	8-week		
Potri. 013G119400 Potri. 011G096600	*PtoTCP20*	*P. tremloides*	*PtomTCP20*-overexpressing lines	2-mouth	Controls vascular cambium proliferation by binding to *PtoWOX4a* and promotes secondary xylem differentiation by activating *PtoWND6* transcription to regulate secondary growth	[50]
Potri. 018G045100	*PtrHB7*	*P. trichocarpa*	*PtrHB7*-RNAi lines	4-mouth	Critical for controlling the differentiation between secondary xylem and phloem tissues during secondary growth	[48]
Potri. 001G372300 Potri. 011G098300	*PtrHB4*		*PtrHB4* RNAi lines	2-mouth	Required for vascular cambium development	[26]
Potri. 015G077100	*PdeHCA2* (*PdeDof5.6*)	*P. deltoides* × *P. euramericana* 'Nanlin895'	*PdeHCA2*-overexpressing lines	1-mouth	Repressed cambium formation and xylem proliferation and differentiation in a dosage-dependent manner	[51]
Potri. 017G074600	*PttCLE47*	*P. tremula* × *tremuloides*	*PttCLE47*-RNAi lines	10-week	A positive regulator of cambial activity. It also promotes secondary xylem production	[52]
Potri. 008G043900 Potri. 010G217700	*PagLBD3*	*P. alba* × *P. glandulosa*	*PagLBD3*-overexpressing lines *PagLBD3*-SRDX mutants	2-mouth 2-mouth	Involved in cambial cell differentiation into secondary phloem	[46]

3.7. Analysis of Transcription Factors under Drought Stress

Transcription factor (TF) families possessing specific conserved domains play key roles in plant growth, development [53], and responses to drought stress [54]. Among the DEGs identified between the WC versus DC and WX versus DX were 1098 TF genes. Specific to the WC versus DC were 380 TFs (134 upregulated and 246 downregulated), and specific to the WX versus DX were 205 TFs (136 upregulated and 69 downregulated). A total of 513 TFs were common between both groups, with 330 upregulated and 183 downregulated in WC versus DC, and 339 upregulated and 174 downregulated in WX versus DX (Figure 7a). We focused our analysis on the genes from the top ten TF families identified (Figure 7b). A total of 138 *MYB* genes (Figure 7c), 130 *AP2/EREBP* genes (Figure 7d), 89 *bHLH* genes (Figure 7e), and 81 *NAC* genes (Figure 7f) were differentially expressed in the stem xylem and cambium tissues in response to drought. Interestingly, some genes in the *AP2/EREBP* family were upregulated in the xylem and downregulated in the cambium, such as *PtrRAP2.3* and *PtrCRF2*. These results indicated that TF genes in the cambium and xylem play different regulatory roles in response to drought. Most TF genes were downregulated in the cambium in response to drought but upregulated in the xylem (Supplementary Tables S11 and S12). This suggests a coordinated function between different plant tissues during the drought response.

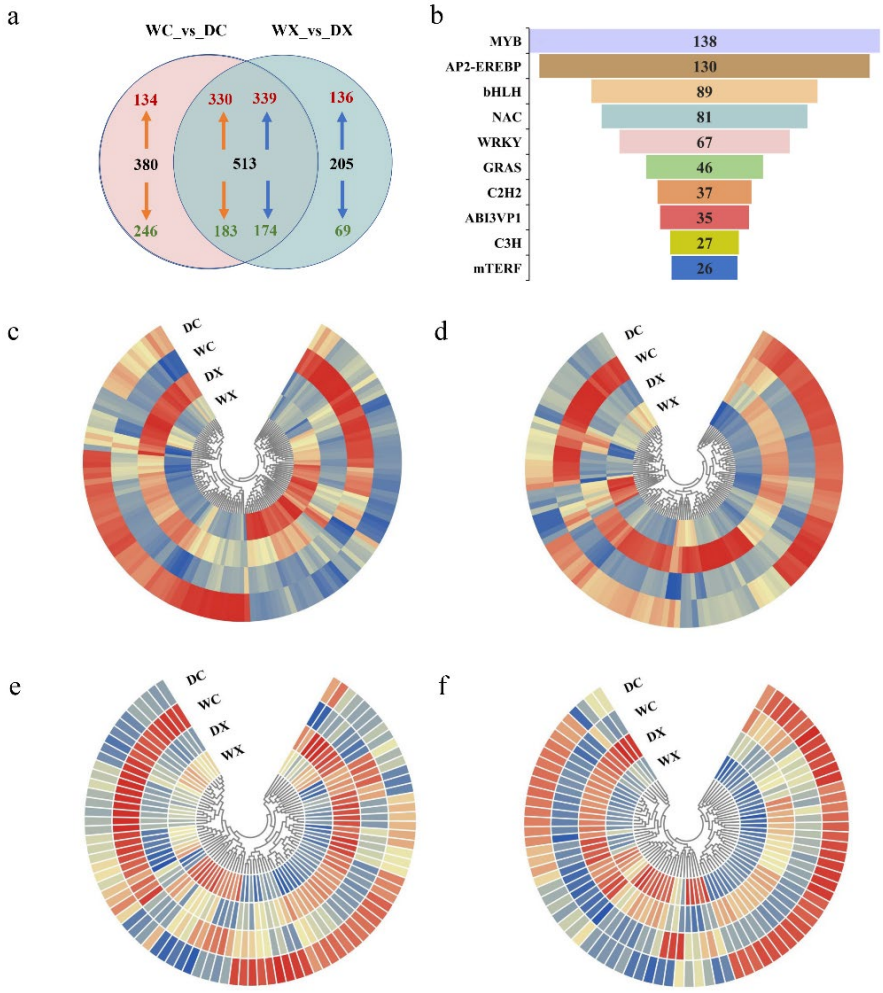

Figure 7. A comparison of differentially expressed transcription factors (TFs) between and within treatment groups. (**a**) A Venn diagram of differentially expressed TFs unique to and shared between the WC versus DC and WX versus DX treatment groups. Pink circle: WC versus DC; blue circle: WX

versus DX. The black number indicates the number of DEGs, the red number indicates the number of upregulated DEGs, and the green number indicates the number of downregulated DEGs annotated as TFs. (**b**) The number of differentially expressed TFs within each of the top ten most abundant TF families. (**c**) Heatmap showing the expression of TFs in the MYB family, (**d**) AP2-EREBP family, (**e**) bHLH family, and (**f**) NAC family. Abbreviations: xylem under control (WX); xylem under drought (DX); cambium under control (WC); cambium under drought (DC). The color scale represents the $\log_2$ fold-change with blue to red, indicating expression values from low to high.

We next analyzed the upregulated TFs from the top four TF families within the WX versus DX (Supplementary Figure S3a) and WC versus DC (Supplementary Figure S3b) groups. The TFs were ranked according to their fold-change increase. The top five TFs with the greatest change in gene expression upon drought treatment for each family were analyzed in greater detail. *MYB102-2*, *NAC047-1*, *NAC047-2*, *NAC072*, *bHLH162-1*, *bHLH162-2*, *ERF114*, and *ERF021-2* had the greatest increase in expression based on a normalized FPKM comparison for each module. These results suggest that these eight TFs are intimately associated with stem xylem development and cambial activity.

3.8. Interaction Networks for Proteins Related to Wood Formation

To better understand the mechanism of wood formation during drought stress, we focused on the eight TFs identified in the previous paragraph. We constructed an interaction network of proteins with functions related to plant hormone signal transduction and amino sugar and nucleotide sugar metabolism (Figure 8a). The proteins' physical interactions between NAC047, NAC072, and MYB102 were closely related to plant hormone signal transduction. MYB102 directly interacted with ABF2, NAC072 directly interacted with BZR1 and MYC2, and NAC047 and NAC072 directly interacted with EIN3. Interestingly, MYC2 and EIN3 directly interacted with PAL1, which is involved in monolignol biosynthesis. Monolignol, cellulose, and hemicellulose biosynthesis-related proteins are closely related to sugar metabolism pathway proteins. Meanwhile, ERF021 directly interacted with LBD1 and LBD4, which are proteins involved in the regulation of cambium activity, and the cambium activity-related proteins are closely related to the proteins involved in plant hormone signal transduction. To support these results, we verified the expression of the TFs in the xylem and cambium under drought stress using RT-qPCR (Figure 8b). The results showed that *PtrERF021-2* was significantly upregulated in the cambium under drought, and *PtrMYB102-2*, *PtrNAC047-1*, *PtrNAC047-2*, and *PtrNAC072* were significantly upregulated in the xylem under drought. Therefore, we concluded that *PtrERF021-2*, *PtrMYB102-2*, *PtrNAC047-1*, *PtrNAC047-2*, and *PtrNAC072* played important roles in wood formation by regulating the hormone signal transduction and amino sugar and nucleotide sugar metabolisms under drought stress.

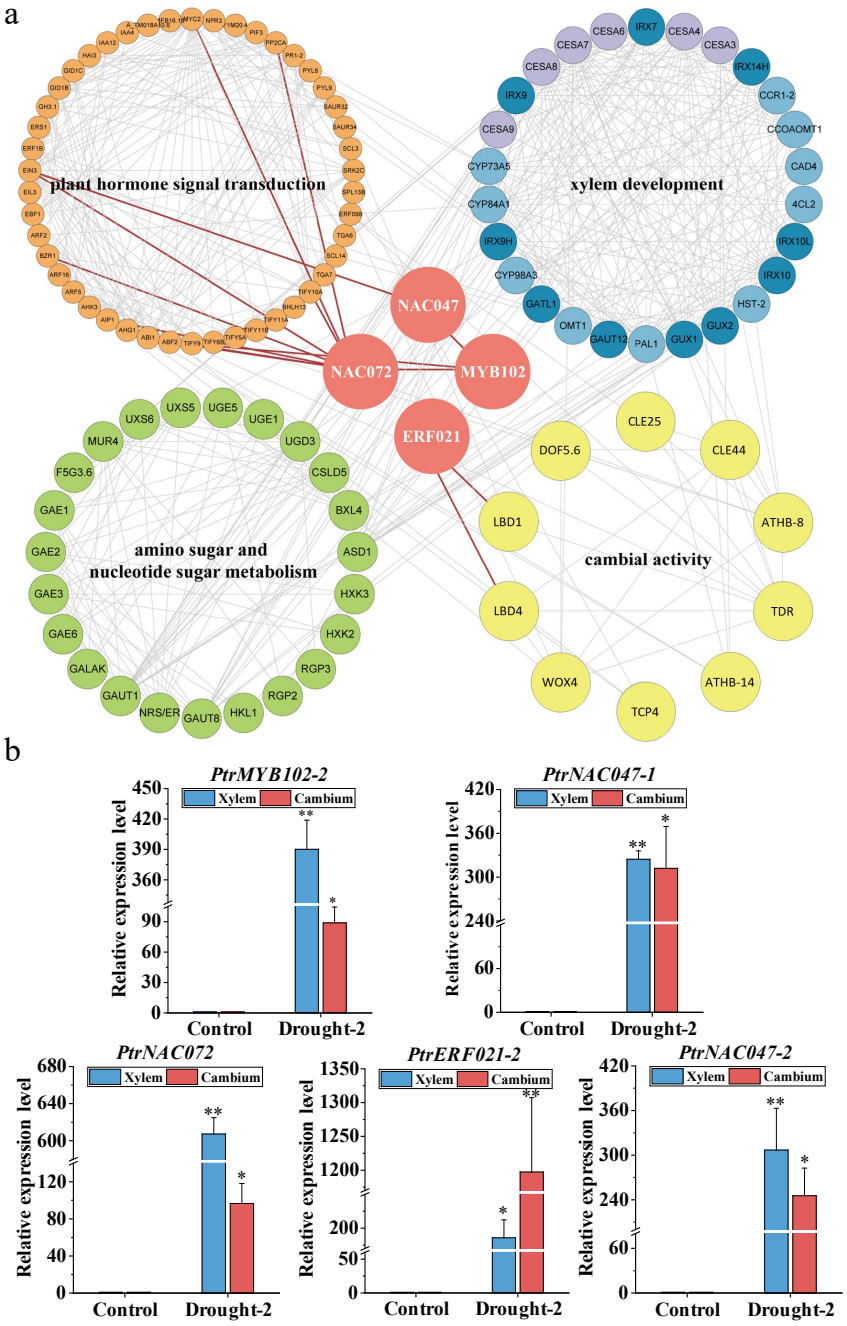

Figure 8. An analysis of the interactions between structural genes and transcription factors (TFs) and their expression patterns. (**a**) An interaction network map of TFs and proteins related to xylem development, cambial activity, plant hormone signal transduction, and sugar metabolism. (**b**) RT-qPCR results show the expression level of five TF genes in stem xylem and cambium tissue. The *Y*-axis on the left indicates the relative gene expression levels, and the *X*-axis represents the two treatment types. Error bars indicate the mean ± SE ($n = 3$) from three independent experiments. A two-tailed Student's *t*-test was used to assess statistical significance. * $p < 0.05$ and ** $p < 0.01$.

4. Discussion

In woody plants, wood formation is a significant part of the plant's growth, involving complex regulatory mechanisms and abiotic stress adaptation [55,56]. In this study, we analyzed the gene expression changes in hormone, metabolic, and biosynthetic pathways during CPD, CE, SCW thickening, and PCD in stem xylem and cambium tissues under drought stress. Studying gene expression changes in hormone, metabolic, and biosynthetic

pathways during different stages of stem development under drought stress provides valuable insights into how plants respond and adapt to environmental challenges. By elucidating the molecular mechanisms associated with these processes, we can better understand the regulatory networks involved in drought responses and potentially identify the key genes or pathways that can be targeted for improving drought tolerance in crop plants, leading to more resilient agricultural systems in the face of climate change.

4.1. Drought Stress Interferes with Stem Growth and Development in P. trichocarpa

We used the model woody plant *P. trichocarpa* to explore the molecular mechanism of wood formation in response to short-term drought, consisting of a SWC of 19%. Studies have shown that drought greatly impacts the production of secondary metabolites in roots [57], photosynthesis in leaves [58], and water transport in stems [59]. We found that severe short-term drought causes obvious phenotypic changes in the growth of leaves and stems (Figure 1a,c). As the soil VWC declines (Figure 1b), stems lose water and become blocked during water transport (Figure 1d,e). This could be the result of changes in the recycling photosynthesis in the stem [60] and the size and number of vessels in the xylem [61]. We observed that the number of vessel cells in the xylem increases during drought, whereas the average area of each vessel cell actually decreases (Figure 2a,c–e). The amount of lignin deposited in the cell wall of the fiber cells increases upon drought stress (Figure 2b). The number of cambium cell layers between internodes was one or two fewer under the drought conditions compared to the control conditions (Figure 2b). These results are consistent with previous studies of xylem in *Populus tomentosa* [62] and cambium in *P. trichocarpa* [63].

4.2. Drought Stress Disrupts Plant Hormone Signal Transduction and Carbohydrate Metabolism during Wood Formation

During wood formation under non-stressed conditions, CPD in the stem cambium is regulated by plant hormones and genes related to cambial activity [64], but how this process is affected by drought stress is less understood. Plant hormones play an important role in regulating vascular cambial activity and plant responses to drought [65]. For example, cytokinin and brassinosteroid play important regulatory roles in cambium cell proliferation [66,67], while auxin promotes the differentiation of cambial cells into xylem [68]. The PP2A phosphatase binds to PIN proteins directly to affect auxin transport. ABA inhibits PP2A phosphatase activity after binding to the PYR/PYL receptors, which results in a greater abundance of phosphorylated PIN proteins that affect auxin transport [69]. Interestingly, we found that the genes involved in plant hormone signal transduction were enriched during drought stress (Figure 3a–f). Most of the genes involved in ABA transport were significantly upregulated under drought stress. This included the *PP2C* genes, which were more highly upregulated than others. Other hormone pathways were also clearly impacted by drought in the cambium (Figure 4).

The expression patterns of the genes related to cambial activity also changed in the cambium under drought stress (Supplementary Figure S2), which showed that most genes were downregulated, except for *LBD3a*, *VCM1*, *VCM2*, and *DA1*. Briefly, CPD in the cambium during wood formation is inhibited under drought stress, including the transduction of plant hormone signals and the regulation of the genes related to cambial activity.

For the processes involving CE, SCW, and PCD in the stem xylem, cell wall biosynthesis determines xylem development, which includes the primary and secondary cell walls [70]. However, drought led to impaired xylem development and affected the expression of the genes related to lignin biosynthesis. Previous studies have demonstrated that drought stress increases the percentage of transcripts with long poly (A) tails in the stem-differentiating xylem of *P. trichocarpa* [55,56]. The cellulose and hemicellulose contents of the primary cell wall during CE [71] are regulated by the genes related to cellulose and hemicellulose biosynthesis. For example, *CesA* genes encode proteins that combine to form functional CESA complexes that are active during SCW thickening [72]. Genes related

to cellulose (Figure 6b) and hemicellulose (Figure 6c) biosynthesis in the xylem of *P. trichocarpa* [14,73] were primarily downregulated during drought (Supplementary Figure S1). The expression patterns of most genes in the monolignol biosynthesis pathway were downregulated in response to drought (Figure 6a). UDP-sugar is a substrate for polysaccharides, so the metabolic pathway involved in UDP-sugar biosynthesis also plays an important role during cell wall biosynthesis [74]. Although the metabolic pathway of UDP-sugar is involved in complex reactions, the metabolic process was limited by the expression pattern analysis of the DEGs related to UDP-sugar metabolism (Figure 5). We found that the genes related to PCD were slightly downregulated by drought in the xylem (Supplementary Table S13) [75–77]. This is despite the fact that many nucleases and proteases are present in tracheary elements [78]. The xylem of *P. trichocarpa* during wood formation under drought stress exhibits problems with primary cell wall formation, accelerated SCW thickening, and changes in the biosynthesis of lignin, cellulose, hemicellulose, and UDP-sugar metabolism.

4.3. Molecular Regulation of Wood Formation in Response to Drought Stress

TFs are important regulators of plant growth, development, and tolerance to drought stress [79]. Specifically, MYB TFs are involved in the drought stress response in *P. trichocarpa* and *P. tomentosa* [80,81]. In this study, we identified 10 TF families consisting of hundreds of DEGs in the cambium and xylem under drought stress (Figure 7b). The MYB, AP2, bHLH, and NAC families had the most DEGs (Figure 7c–f). The TFs in these four families are known to promote tolerance against drought by regulating secondary growth in *Oryza sativa* [82], *Sorghum bicolor* [83], *Betula platyphylla* [84], *Vitis vinifera* L. [85], and *Apium graveolens* L. [86]. MYB and NAC TFs, in particular, regulate secondary cell wall biosynthesis [4]. For instance, wood-associated NAC domain (WND) TFs are part of a hierarchical network regulating wood formation in woody plants. Alternatively, spliced isoforms of *PtrWND1B* are negative regulators of fiber cell wall thickening during wood formation [87]. The PtrMYB74-PtrWRKY19-PtrbHLH186 network also plays a vital role in regulating wood formation in addition to promoting drought tolerance in plants [36].

We identified eight TFs that might play critical roles during wood formation (Supplementary Figure S3) and selected five TFs (PtrMYB102-2, PtrNAC047-1, PtrNAC047-2, PtrNAC072, and PtrERF021-2) by analyzing the interaction network among the genes related to xylem development and cambial activity (Figure 8b). An *Arabidopsis thaliana atnac029/atnac047/atnac092* triple mutant exhibited delayed ovule degeneration [88]. *AtNAC072* (*RD26*) is a key regulator of metabolic reprogramming during dark-induced senescence [89], which plays an important role in regulating ABA signal transduction in response to drought [90,91]. *AtMYB102* expression was rapidly induced by osmotic stress and ABA treatment and depends on and integrates signals derived from both wounding and osmotic stress [92]. We believe that PtrMYB102-2, PtrNAC047-1, PtrNAC047-2, and PtrNAC072 may regulate lignin deposition and PCD to accelerate xylem development in response to drought stress. These proteins likely accomplish this by interacting with proteins related to lignin, cellulose, and hemicellulose biosynthesis and sugar metabolism (Figure 8a). *AtERF021* (*FUF1*) suppresses the Ethylene response DNA-binding Factors (EDFs) that promote floral senescence/abscission by regulating ethylene signal transduction [93]. We believe that PtrERF021-2 may regulate cambium activity in response to drought stress by interacting with the proteins related to plant hormone signal transduction (Figure 8a). In summary, TFs such as *PtrMYB102-2*, *PtrNAC047-1*, *PtrNAC047-2*, *PtrNAC072*, and *PtrERF021-2* are differentially expressed under drought conditions and interact with the proteins involved in plant hormone signal transduction and the amino sugar and nucleotide sugar metabolisms. As a result, wood formation is affected. The genes related to cambium activity (*WOX4*, *VCM1/2*, and *LBD4*), xylem development (*CesAs*, *GUX1a/b*, *IRXs*, *PARVUS-L-1*, *PALs*, *4CLs*, and *COMTs*), vacuole collapse, and cell autolysis (*XCP1/2*, *MC9*, and *APX*) also undergo expression changes during drought stress. These changes in gene expression affect CPD, CE, SCW, and PCD to influence wood formation (Figure 9).

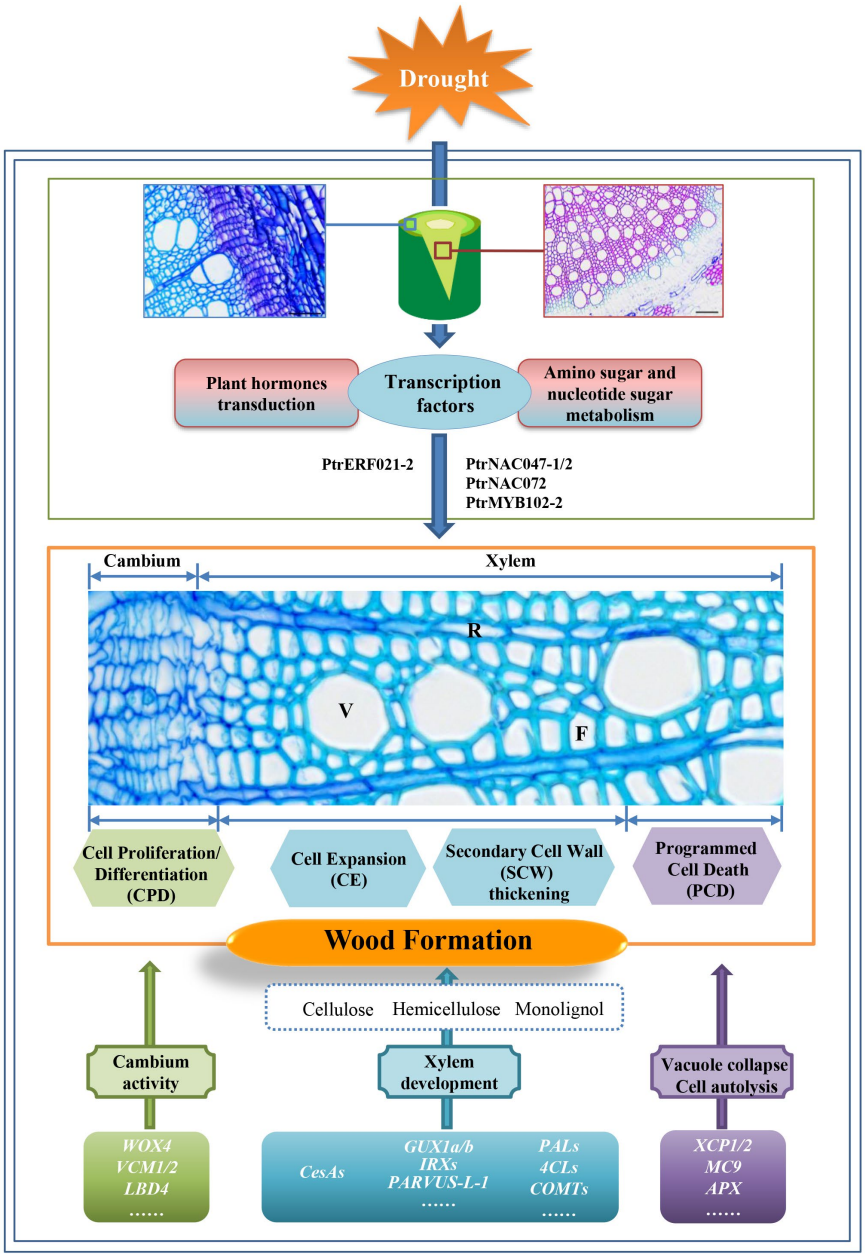

Figure 9. Schematic summary of changes in gene expression during wood formation under drought stress. V: vessel cells; F: fiber cells; R: ray cells.

5. Conclusions

We analyzed the changes in gene expression during wood formation under drought stress in *P. trichocarpa*. PtrERF021-2 modulates cambium activity in the stem by regulating plant hormone signal transduction to suppress CPD. PtrMYB102, PtrNAC47-1, PtrNAC47-2, and PtrNAC072 modulate xylem development in the stem by regulating lignin, cellulose, and hemicellulose biosynthesis and sugar metabolism in response to drought stress to suppress CE and SCW thickening. The effects of drought stress on wood formation are complex. This is particularly true for the effects of drought on CPD, CE, SCW thickening, and PCD in the stem xylem and cambium. In future studies, we will focus on uncovering new details about the role played by TFs in wood formation during drought stress and the gene networks they regulate.

Supplementary Materials: The following supporting information can be downloaded at: https://www.mdpi.com/article/10.3390/f15050873/s1.

Author Contributions: Conceptualization, C.L. and G.Q.; Formal analysis, L.D.; Methodology, B.C. and T.W.; Project administration, G.Q.; Software, X.L. and D.Z.; Supervision, C.L. and G.Q.; Resources, G.Q.; Writing—original draft, L.D.; Writing—review and editing, L.D. All authors have read and agreed to the published version of the manuscript.

Funding: This research was funded by the Heilongjiang Province Key Research and Development Program of China (GA21B010) and the Fundamental Research Funds for the Central Universities (2572023CT19).

Data Availability Statement: The RNA-seq data have been deposited in the National Center for Biotechnology Information Sequence Read Archive under accession number PRJNA901629.

Conflicts of Interest: The authors declare no conflicts of interest.

References

1. Evert, R.F. *Esau's Plant Anatomy: Meristems, Cells, and Tissues of the Plant Body: Their Structure, Function, and Development*; John Wiley & Sons: Hoboken, NJ, USA, 2006. [CrossRef]
2. Mizrachi, E.; Maloney, V.J.; Silberbauer, J.; Hefer, C.A.; Berger, D.K.; Mansfield, S.D.; Myburg, A.A. Investigating the molecular underpinnings underlying morphology and changes in carbon partitioning during tension wood formation in *Eucalyptus*. *New Phytol.* **2014**, *206*, 1351–1363. [CrossRef]
3. Plomion, C.; Leprovost, G.; Stokes, A. Wood Formation in Trees. *Plant Physiol.* **2001**, *127*, 1513–1523. [CrossRef]
4. Luo, L.; Li, L. Molecular understanding of wood formation in trees. *For. Res.* **2022**, *2*, 5. [CrossRef]
5. Zheng, S.; He, J.; Lin, Z.; Zhu, Y.; Sun, J.; Li, L. Two MADS-box genes regulate vascular cambium activity and secondary growth by modulating auxin homeostasis in *Populus*. *Plant Commun.* **2021**, *2*, 100134. [CrossRef]
6. Di, D.-W.; Zhang, C.; Guo, G.-Q. Involvement of secondary messengers and small organic molecules in auxin perception and signaling. *Plant Cell Rep.* **2015**, *34*, 895–904. [CrossRef]
7. Nilsson, J.; Karlberg, A.; Antti, H.; Lopez-Vernaza, M.; Mellerowicz, E.; Perrot-Rechenmann, C.; Sandberg, G.r.; Bhalerao, R.P. Dissecting the molecular basis of the regulation of wood formation by auxin in hybrid aspen. *Plant Cell* **2008**, *20*, 843–855. [CrossRef]
8. Lee, J.; Kim, H.; Park, S.G.; Hwang, H.; Yoo, S.i.; Bae, W.; Kim, E.; Kim, J.; Lee, H.Y.; Heo, T.Y.; et al. Brassinosteroid-BZR1/2-WAT1 module determines the high level of auxin signalling in vascular cambium during wood formation. *New Phytol.* **2021**, *230*, 1503–1516. [CrossRef]
9. Shi, R.; Wang, J.P.; Lin, Y.-C.; Li, Q.; Sun, Y.-H.; Chen, H.; Sederoff, R.R.; Chiang, V.L. Tissue and cell-type co-expression networks of transcription factors and wood component genes in *Populus trichocarpa*. *Planta* **2017**, *245*, 927–938. [CrossRef]
10. Abedi, T.; Castilleux, R.; Nibbering, P.; Niittylä, T. The Spatio-Temporal Distribution of Cell Wall-Associated Glycoproteins During Wood Formation in *Populus*. *Front. Plant Sci.* **2020**, *11*, 611607. [CrossRef]
11. Loziuk, P.L.; Parker, J.; Li, W.; Lin, C.-Y.; Wang, J.P.; Li, Q.; Sederoff, R.R.; Chiang, V.L.; Muddiman, D.C. Elucidation of Xylem-Specific Transcription Factors and Absolute Quantification of Enzymes Regulating Cellulose Biosynthesis in *Populus trichocarpa*. *J. Proteome Res.* **2015**, *14*, 4158–4168. [CrossRef]
12. Vanholme, R.; Demedts, B.; Morreel, K.; Ralph, J.; Boerjan, W. Lignin Biosynthesis and Structure. *Plant Physiol.* **2010**, *153*, 895–905. [CrossRef]
13. Yoo, C.G.; Dumitrache, A.; Muchero, W.; Natzke, J.; Akinosho, H.; Li, M.; Sykes, R.W.; Brown, S.D.; Davison, B.; Tuskan, G.A.; et al. Significance of Lignin S/G Ratio in Biomass Recalcitrance of *Populus trichocarpa* Variants for Bioethanol Production. *ACS Sustain. Chem. Eng.* **2017**, *6*, 2162–2168. [CrossRef]
14. Wang, J.P.; Matthews, M.L.; Williams, C.M.; Shi, R.; Yang, C.; Tunlaya-Anukit, S.; Chen, H.-C.; Li, Q.; Liu, J.; Lin, C.-Y.; et al. Improving wood properties for wood utilization through multi-omics integration in lignin biosynthesis. *Nat. Commun.* **2018**, *9*, 1579. [CrossRef]
15. Wang, J.P.; Naik, P.P.; Chen, H.-C.; Shi, R.; Lin, C.-Y.; Liu, J.; Shuford, C.M.; Li, Q.; Sun, Y.-H.; Tunlaya-Anukit, S.; et al. Complete proteomic-based enzyme reaction and inhibition kinetics reveal how monolignol biosynthetic enzyme families affect metabolic flux and lignin in *Populus trichocarpa*. *Plant Cell* **2014**, *26*, 894–914. [CrossRef]
16. Lin, C.-Y.; Sun, Y.; Song, J.; Chen, H.-C.; Shi, R.; Yang, C.; Liu, J.; Tunlaya-Anukit, S.; Liu, B.; Loziuk, P.L.; et al. Enzyme Complexes of Ptr4CL and PtrHCT Modulate Co-enzyme A Ligation of Hydroxycinnamic Acids for Monolignol Biosynthesis in *Populus trichocarpa*. *Front. Plant Sci.* **2021**, *12*, 727932. [CrossRef]
17. De Roo, L.; Salomón, R.L.; Oleksyn, J.; Steppe, K. Woody tissue photosynthesis delays drought stress in *Populus tremula* trees and maintains starch reserves in branch xylem tissues. *New Phytol.* **2020**, *228*, 70–81. [CrossRef]
18. Dox, I.; Prislan, P.; Gričar, J.; Mariën, B.; Delpierre, N.; Flores, O.; Leys, S.; Rathgeber, C.B.K.; Fonti, P.; Campioli, M. Drought elicits contrasting responses on the autumn dynamics of wood formation in late successional deciduous tree species. *Tree Physiol.* **2021**, *41*, 1171–1185. [CrossRef]

19. Fischer, U.; Kucukoglu, M.; Helariutta, Y.; Bhalerao, R.P. The Dynamics of Cambial Stem Cell Activity. *Annu. Rev. Plant Biol.* **2019**, *70*, 293–319. [CrossRef]
20. Yang, X.; Lu, M.; Wang, Y.; Wang, Y.; Liu, Z.; Chen, S. Response Mechanism of Plants to Drought Stress. *Horticulturae* **2021**, *7*, 50. [CrossRef]
21. Kuromori, T.; Fujita, M.; Takahashi, F.; Yamaguchi-Shinozaki, K.; Shinozaki, K. Inter-tissue and inter-organ signaling in drought stress response and phenotyping of drought tolerance. *Plant J.* **2021**, *109*, 342–358. [CrossRef]
22. Han, X.; Zhao, Y.; Chen, Y.; Xu, J.; Jiang, C.; Wang, X.; Zhuo, R.; Lu, M.-Z.; Zhang, J. Lignin biosynthesis and accumulation in response to abiotic stresses in woody plants. *For. Res.* **2022**, *2*, 9. [CrossRef]
23. Chao, N.; Huang, S.; Kang, X.; Yidilisi, K.; Dai, M.; Liu, L. Systematic functional characterization of cinnamyl alcohol dehydrogenase family members revealed their functional divergence in lignin biosynthesis and stress responses in mulberry. *Plant Physiol. Biochem.* **2022**, *186*, 145–156. [CrossRef]
24. Song, J.-L.; Wang, Z.-Y.; Wang, Y.-H.; Du, J.; Wang, C.-Y.; Zhang, X.-Q.; Chen, S.; Huang, X.-L.; Xie, X.-M.; Zhong, T.-X. Overexpression of *Pennisetum purpureum CCoAOMT* Contributes to Lignin Deposition and Drought Tolerance by Promoting the Accumulation of Flavonoids in Transgenic Tobacco. *Front. Plant Sci.* **2022**, *13*, 884456. [CrossRef]
25. Chen, Y.; Yordanov, Y.S.; Ma, C.; Strauss, S.; Busov, V.B. DR5 as a reporter system to study auxin response in *Populus*. *Plant Cell Rep.* **2013**, *32*, 453–463. [CrossRef]
26. Zhu, Y.; Song, D.; Xu, P.; Sun, J.; Li, L. A *HD-ZIP III* gene, *PtrHB4*, is required for interfascicular cambium development in *Populus*. *Plant Biotechnol. J.* **2018**, *16*, 808–817. [CrossRef]
27. Chen, J.J.; Wang, L.Y.; Immanen, J.; Nieminen, K.; Spicer, R.; Helariutta, Y.; Zhang, J.; He, X.Q. Differential regulation of auxin and cytokinin during the secondary vascular tissue regeneration in *Populus* trees. *New Phytol.* **2019**, *224*, 188–201. [CrossRef]
28. Mauriat, M.; Sandberg, L.G.; Moritz, T. Proper gibberellin localization in vascular tissue is required to control auxin-dependent leaf development and bud outgrowth in hybrid aspen. *Plant J.* **2011**, *67*, 805–816. [CrossRef]
29. Park, E.-J.; Kim, H.-T.; Choi, Y.-I.; Lee, C.; Nguyen, V.P.; Jeon, H.-W.; Cho, J.-S.; Pharis, R.P.; Kurepin, L.V.; Ko, J.-H.; et al. Overexpression of gibberellin *20-oxidase1* from *Pinus densiflora* results in enhanced wood formation with gelatinous fiber development in a transgenic hybrid poplar. *Tree Physiol.* **2015**, *35*, 1264–1277. [CrossRef]
30. Bajguz, A. Metabolism of brassinosteroids in plants. *Plant Physiol. Biochem.* **2007**, *45*, 95–107. [CrossRef]
31. Love, J.; Björklund, S.; Vahala, J.; Hertzberg, M.; Kangasjärvi, J.; Sundberg, B. Ethylene is an endogenous stimulator of cell division in the cambial meristem of *Populus*. *Proc. Natl. Acad. Sci. USA* **2009**, *106*, 5984–5989. [CrossRef]
32. Pearce, D.W.; Rood, S.B.; Wu, R. Phytohormones and shoot growth in a three-generation hybrid poplar family. *Tree Physiol.* **2004**, *24*, 217–224. [CrossRef]
33. Wei, H.; Gou, J.; Yordanov, Y.; Zhang, H.; Thakur, R.; Jones, W.; Burton, A. Global transcriptomic profiling of aspen trees under elevated [CO_2] to identify potential molecular mechanisms responsible for enhanced radial growth. *J. Plant Res.* **2012**, *126*, 305–320. [CrossRef]
34. Waadt, R.; Seller, C.A.; Hsu, P.-K.; Takahashi, Y.; Munemasa, S.; Schroeder, J.I. Plant hormone regulation of abiotic stress responses. *Nat. Rev. Mol. Cell Biol.* **2022**, *23*, 680–694. [CrossRef]
35. Li, S.; Lin, Y.-C.J.; Wang, P.; Zhang, B.; Li, M.; Chen, S.; Shi, R.; Tunlaya-Anukit, S.; Liu, X.; Wang, Z.; et al. The AREB1 Transcription Factor Influences Histone Acetylation to Regulate Drought Responses and Tolerance in *Populus trichocarpa*. *Plant Cell* **2019**, *31*, 663–686. [CrossRef]
36. Liu, H.; Gao, J.; Sun, J.; Li, S.; Zhang, B.; Wang, Z.; Zhou, C.; Sulis, D.B.; Wang, J.P.; Chiang, V.L.; et al. Dimerization of PtrMYB074 and PtrWRKY19 mediates transcriptional activation of *PtrbHLH186* for secondary xylem development in *Populus trichocarpa*. *New Phytol.* **2022**, *234*, 918–933. [CrossRef]
37. Li, M.; Dong, H.; Li, J.; Dai, X.; Lin, J.; Li, S.; Zhou, C.; Chiang, V.L.; Li, W. *PtrVCS2* Regulates Drought Resistance by Changing Vessel Morphology and Stomatal Closure in *Populus trichocarpa*. *Int. J. Mol. Sci.* **2023**, *24*, 4458. [CrossRef]
38. Langmead, B.; Salzberg, S.L. Fast gapped-read alignment with Bowtie 2. *Nat. Methods* **2012**, *9*, 357–359. [CrossRef]
39. Wang, L.; Feng, Z.; Wang, X.; Wang, X.; Zhang, X. DEGseq: An R package for identifying differentially expressed genes from RNA-seq data. *Bioinformatics* **2010**, *26*, 136–138. [CrossRef]
40. Livak, K.J.; Schmittgen, T.D. Analysis of relative gene expression data using real-time quantitative PCR and the 2(-Delta Delta C(T)) Method. *Methods* **2001**, *25*, 402–408. [CrossRef]
41. Haas, A.S.; Shi, D.; Greb, T. Cell Fate Decisions Within the Vascular Cambium–Initiating Wood and Bast Formation. *Front. Plant Sci.* **2022**, *13*, 864422. [CrossRef]
42. Milhinhos, A.; Miguel, C.M. Hormone interactions in xylem development: A matter of signals. *Plant Cell Rep.* **2013**, *32*, 867–883. [CrossRef]
43. Sakamoto, S.; Somssich, M.; Nakata, M.T.; Unda, F.; Atsuzawa, K.; Kaneko, Y.; Wang, T.; Bågman, A.-M.; Gaudinier, A.; Yoshida, K.; et al. Complete substitution of a secondary cell wall with a primary cell wall in Arabidopsis. *Nat. Plants* **2018**, *4*, 777–783. [CrossRef]
44. Secchi, F.; Gilbert, M.E.; Zwieniecki, M.A. Transcriptome Response to Embolism Formation in Stems of *Populus trichocarpa* Provides Insight into Signaling and the Biology of Refilling. *Plant Physiol.* **2011**, *157*, 1419–2945. [CrossRef]

45. Takata, N.; Awano, T.; Nakata, M.T.; Sano, Y.; Sakamoto, S.; Mitsuda, N.; Taniguchi, T.; Tsai, C.-J. Populus NST/SND orthologs are key regulators of secondary cell wall formation in wood fibers, phloem fibers and xylem ray parenchyma cells. *Tree Physiol.* **2019**, *39*, 514–525. [CrossRef]
46. Han, Z.; Yang, T.; Guo, Y.; Cui, W.-H.; Yao, L.-J.; Li, G.; Wu, A.-M.; Li, J.-H.; Liu, L.-J.; Liesche, J. The transcription factor PagLBD3 contributes to the regulation of secondary growth in *Populus*. *J. Exp. Bot.* **2021**, *72*, 7092–7106. [CrossRef]
47. Tang, X.; Wang, C.; Chai, G.; Wang, D.; Xu, H.; Liu, Y.; He, G.; Liu, S.; Zhang, Y.; Kong, Y.; et al. Ubiquitinated DA1 negatively regulates vascular cambium activity through modulating the stability of WOX4 in *Populus*. *Plant Cell* **2022**, *34*, 3364–3382. [CrossRef]
48. Zhu, Y.; Song, D.; Sun, J.; Wang, X.; Li, L. *PtrHB7*, a class III HD-Zip Gene, Plays a Critical Role in Regulation of Vascular Cambium Differentiation in *Populus*. *Mol. Plant* **2013**, *6*, 1331–1343. [CrossRef]
49. Smit, M.E.; McGregor, S.R.; Sun, H.; Gough, C.; Bågman, A.-M.; Soyars, C.L.; Kroon, J.T.; Gaudinier, A.; Williams, C.J.; Yang, X.; et al. A PXY-Mediated Transcriptional Network Integrates Signaling Mechanisms to Control Vascular Development in Arabidopsis. *Plant Cell* **2020**, *32*, 319–335. [CrossRef]
50. Hou, J.; Xu, H.; Fan, D.; Ran, L.; Li, J.; Wu, S.; Luo, K.; He, X.Q. MiR319a-targeted *PtoTCP20* regulates secondary growth via interactions with PtoWOX4 and *PtoWND6* in *Populus tomentosa*. *New Phytol.* **2020**, *228*, 1354–1368. [CrossRef]
51. Zhao, B.-G.; Li, G.; Wang, Y.-F.; Yan, Z.; Dong, F.-Q.; Mei, Y.-C.; Zeng, W.; Lu, M.-Z.; Li, H.-B.; Chao, Q.; et al. *PdeHCA2* affects biomass in *Populus* by regulating plant architecture, the transition from primary to secondary growth, and photosynthesis. *Planta* **2022**, *255*, 101. [CrossRef]
52. Kucukoglu, M.; Chaabouni, S.; Zheng, B.; Mähönen, A.P.; Helariutta, Y.; Nilsson, O. Peptide encoding *Populus CLV3/ESR-RELATED 47* (*PttCLE47*) promotes cambial development and secondary xylem formation in hybrid aspen. *New Phytol.* **2019**, *226*, 75–85. [CrossRef]
53. Pratyusha, D.S.; Sarada, D.V.L. MYB transcription factors-master regulators of phenylpropanoid biosynthesis and diverse developmental and stress responses. *Plant Cell Rep.* **2022**, *41*, 2245–2260. [CrossRef]
54. Wang, B.; Li, S.; Zou, L.; Guo, X.; Liang, J.; Liao, W.; Peng, M. Natural variation *MeMYB108* associated with tolerance to stress-induced leaf abscission linked to enhanced protection against reactive oxygen species in cassava. *Plant Cell Rep.* **2022**, *41*, 1573–1587. [CrossRef]
55. Yu, D.; Janz, D.; Zienkiewicz, K.; Herrfurth, C.; Feussner, I.; Chen, S.; Polle, A. Wood Formation under Severe Drought Invokes Adjustment of the Hormonal and Transcriptional Landscape in Poplar. *Int. J. Mol. Sci.* **2021**, *22*, 9899. [CrossRef]
56. Gao, Y.; Liu, X.; Jin, Y.; Wu, J.; Li, S.; Li, Y.; Chen, B.; Zhang, Y.; Wei, L.; Li, W.; et al. Drought induces epitranscriptome and proteome changes in stem-differentiating xylem of *Populus trichocarpa*. *Plant Physiol.* **2022**, *190*, 459–479. [CrossRef]
57. Li, D.; Yang, J.; Pak, S.; Zeng, M.; Sun, J.; Yu, S.; He, Y.; Li, C. PuC3H35 confers drought tolerance by enhancing lignin and proanthocyanidin biosynthesis in the roots of *Populus ussuriensis*. *New Phytol.* **2021**, *233*, 390–408. [CrossRef]
58. Wang, X.; Du, T.; Huang, J.; Peng, S.; Xiong, D. Leaf hydraulic vulnerability triggers the decline in stomatal and mesophyll conductance during drought in rice. *J. Exp. Bot.* **2018**, *69*, 4033–4045. [CrossRef]
59. Baert, A.; De Schepper, V.; Steppe, K. Variable hydraulic resistances and their impact on plant drought response modelling. *Tree Physiol.* **2014**, *35*, 439–449. [CrossRef]
60. Cernusak, L.A.; Cheesman, A.W. The benefits of recycling: How photosynthetic bark can increase drought tolerance. *New Phytol.* **2015**, *208*, 995–997. [CrossRef]
61. Hori, C.; Yu, X.; Mortimer, J.C.; Sano, R.; Matsumoto, T.; Kikuchi, J.; Demura, T.; Ohtani, M. Impact of abiotic stress on the regulation of cell wall biosynthesis in *Populus trichocarpa*. *Plant Biotechnol.* **2020**, *37*, 273–283. [CrossRef]
62. Kong, L.; Song, Q.; Wei, H.; Wang, Y.; Lin, M.; Sun, K.; Zhang, Y.; Yang, J.; Li, C.; Luo, K. The AP2/ERF transcription factor PtoERF15 confers drought tolerance via JA-mediated signaling in *Populus*. *New Phytol.* **2023**, *240*, 1848–1867. [CrossRef]
63. Dai, X.; Zhai, R.; Lin, J.; Wang, Z.; Meng, D.; Li, M.; Mao, Y.; Gao, B.; Ma, H.; Zhang, B.; et al. Cell-type-specific PtrWOX4a and PtrVCS2 form a regulatory nexus with a histone modification system for stem cambium development in *Populus trichocarpa*. *Nat. Plants* **2023**, *9*, 96–111. [CrossRef]
64. Wang, D.; Chen, Y.; Li, W.; Li, Q.; Lu, M.; Zhou, G.; Chai, G. Vascular Cambium: The Source of Wood Formation. *Front. Plant Sci.* **2021**, *12*, 700928. [CrossRef]
65. De Zelicourt, A.; Colcombet, J.; Hirt, H. The Role of MAPK Modules and ABA during Abiotic Stress Signaling. *Trends Plant Sci.* **2016**, *21*, 677–685. [CrossRef]
66. Miyashima, S.; Sebastian, J.; Lee, J.-Y.; Helariutta, Y. Stem cell function during plant vascular development. *EMBO J.* **2012**, *32*, 178–193. [CrossRef]
67. Du, J.; Gerttula, S.; Li, Z.; Zhao, S.T.; Liu, Y.L.; Liu, Y.; Lu, M.Z.; Groover, A.T. Brassinosteroid regulation of wood formation in poplar. *New Phytol.* **2019**, *225*, 1516–1530. [CrossRef]
68. Smetana, O.; Mäkilä, R.; Lyu, M.; Amiryousefi, A.; Sánchez Rodríguez, F.; Wu, M.-F.; Solé-Gil, A.; Leal Gavarrón, M.; Siligato, R.; Miyashima, S.; et al. High levels of auxin signalling define the stem-cell organizer of the vascular cambium. *Nature* **2019**, *565*, 485–489. [CrossRef]

69. Li, Y.; Wang, Y.; Tan, S.; Li, Z.; Yuan, Z.; Glanc, M.; Domjan, D.; Wang, K.; Xuan, W.; Guo, Y.; et al. Root Growth Adaptation is Mediated by PYLs ABA Receptor-PP2A Protein Phosphatase Complex. *Adv. Sci.* **2019**, *7*, 1901455. [CrossRef]
70. Li, W.; Lin, Y.-C.J.; Chen, Y.-L.; Zhou, C.; Li, S.; De Ridder, N.; Oliveira, D.M.; Zhang, L.; Zhang, B.; Wang, J.P.; et al. Woody plant cell walls: Fundamentals and utilization. *Mol. Plant* **2024**, *17*, 112–140. [CrossRef] [PubMed]
71. Cosgrove, D.J.; Jarvis, M.C. Comparative structure and biomechanics of plant primary and secondary cell walls. *Front. Plant Sci.* **2012**, *3*, 204. [CrossRef] [PubMed]
72. Watanabe, Y.; Schneider, R.; Barkwill, S.; Gonzales-Vigil, E.; Hill, J.L.; Samuels, A.L.; Persson, S.; Mansfield, S.D. Cellulose synthase complexes display distinct dynamic behaviors during xylem transdifferentiation. *Proc. Natl. Acad. Sci. USA* **2018**, *115*, E6366–E6374. [CrossRef] [PubMed]
73. Suzuki, S.; Li, L.; Sun, Y.-H.; Chiang, V.L. The Cellulose Synthase Gene Superfamily and Biochemical Functions of Xylem-Specific Cellulose Synthase-Like Genes in *Populus trichocarpa*. *Plant Physiol.* **2006**, *142*, 1233–1245. [CrossRef] [PubMed]
74. Zhang, Q.; Shirley, N.J.; Burton, R.A.; Lahnstein, J.; Hrmova, M.; Fincher, G.B. The Genetics, Transcriptional Profiles, and Catalytic Properties of UDP-α-d-Xylose 4-Epimerases from Barley. *Plant Physiol.* **2010**, *153*, 555–568. [CrossRef] [PubMed]
75. Avci, U.; Earl Petzold, H.; Ismail, I.O.; Beers, E.P.; Haigler, C.H. Cysteine proteases XCP1 and XCP2 aid micro-autolysis within the intact central vacuole during xylogenesis in Arabidopsis roots. *Plant J.* **2008**, *56*, 303–315. [CrossRef] [PubMed]
76. Bollhöner, B.; Zhang, B.; Stael, S.; Denancé, N.; Overmyer, K.; Goffner, D.; Van Breusegem, F.; Tuominen, H. Post mortem function of AtMC9 in xylem vessel elements. *New Phytol.* **2013**, *200*, 498–510. [CrossRef] [PubMed]
77. Zhang, J.; Liu, Y.; Li, C.; Yin, B.; Liu, X.; Guo, X.; Zhang, C.; Liu, D.; Hwang, I.; Li, H.; et al. PtomtAPX is an autonomous lignification peroxidase during the earliest stage of secondary wall formation in *Populus tomentosa* Carr. *Nat Plants.* **2022**, *8*, 828–839. [CrossRef] [PubMed]
78. Escamez, S.; Tuominen, H. Contribution of cellular autolysis to tissular functions during plant development. *Curr. Opin. Plant Biol.* **2017**, *35*, 124–130. [CrossRef] [PubMed]
79. Behr, M.; Guerriero, G.; Grima-Pettenati, J.; Baucher, M. A Molecular Blueprint of Lignin Repression. *Trends Plant Sci.* **2019**, *24*, 1052–1064. [CrossRef] [PubMed]
80. Song, Q.; Kong, L.; Yang, X.; Jiao, B.; Hu, J.; Zhang, Z.; Xu, C.; Luo, K.; David-Schwartz, R. PtoMYB142, a poplar R2R3-MYB transcription factor, contributes to drought tolerance by regulating wax biosynthesis. *Tree Physiol.* **2022**, *42*, 2133–2147. [CrossRef]
81. Fang, Q.; Wang, X.; Wang, H.; Tang, X.; Liu, C.; Yin, H.; Ye, S.; Jiang, Y.; Duan, Y.; Luo, K. The poplar R2R3 MYB transcription factor PtrMYB94 coordinates with abscisic acid signaling to improve drought tolerance in plants. *Tree Physiol.* **2020**, *40*, 46–59. [CrossRef]
82. Jung, S.E.; Bang, S.W.; Kim, S.H.; Seo, J.S.; Yoon, H.-B.; Kim, Y.S.; Kim, J.-K. Overexpression of *OsERF83*, a Vascular Tissue-Specific Transcription Factor Gene, Confers Drought Tolerance in Rice. *Int. J. Mol. Sci.* **2021**, *22*, 7656. [CrossRef] [PubMed]
83. Scully, E.D.; Gries, T.; Sarath, G.; Palmer, N.A.; Baird, L.; Serapiglia, M.J.; Dien, B.S.; Boateng, A.A.; Ge, Z.; Funnell-Harris, D.L.; et al. Overexpression of *SbMyb60* impacts phenylpropanoid biosynthesis and alters secondary cell wall composition in *Sorghum bicolor*. *Plant J.* **2016**, *85*, 378–395. [CrossRef] [PubMed]
84. Hu, P.; Zhang, K.; Yang, C. BpNAC012 Positively Regulates Abiotic Stress Responses and Secondary Wall Biosynthesis. *Plant Physiol.* **2019**, *179*, 700–717. [CrossRef] [PubMed]
85. Tu, M.; Wang, X.; Yin, W.; Wang, Y.; Li, Y.; Zhang, G.; Li, Z.; Song, J.; Wang, X. Grapevine *VlbZIP30* improves drought resistance by directly activating *VvNAC17* and promoting lignin biosynthesis through the regulation of three peroxidase genes. *Hortic. Res.* **2020**, *7*, 150. [CrossRef] [PubMed]
86. Duan, A.-Q.; Tao, J.-P.; Jia, L.-L.; Tan, G.-F.; Liu, J.-X.; Li, T.; Chen, L.-Z.; Su, X.-J.; Feng, K.; Xu, Z.-S.; et al. AgNAC1, a celery transcription factor, related to regulation on lignin biosynthesis and salt tolerance. *Genomics* **2020**, *112*, 5254–5264. [CrossRef] [PubMed]
87. Zhao, Y.; Sun, J.; Xu, P.; Zhang, R.; Li, L. Intron-Mediated Alternative Splicing of WOOD-ASSOCIATED NAC TRANSCRIPTION FACTOR1B Regulates Cell Wall Thickening during Fiber Development in *Populus* Species. *Plant Physiol.* **2014**, *164*, 765–776. [CrossRef] [PubMed]
88. Van Durme, M.; Olvera-Carrillo, Y.; Pfeiffer, M.L.; Doll, N.M.; De Winter, F.; Lin, Z.; Nowack, M.K. Fertility loss in senescing Arabidopsis ovules is controlled by the maternal sporophyte via a NAC transcription factor triad. *Proc. Natl. Acad. Sci. USA* **2023**, *120*, e2219868120. [CrossRef] [PubMed]
89. Kamranfar, I.; Xue, G.P.; Tohge, T.; Sedaghatmehr, M.; Fernie, A.R.; Balazadeh, S.; Mueller-Roeber, B. Transcription factor RD26 is a key regulator of metabolic reprogramming during dark-induced senescence. *New Phytol.* **2018**, *218*, 1543–1557. [CrossRef] [PubMed]
90. Khan, I.U.; Ali, A.; Zareen, S.; Khan, H.A.; Lim, C.J.; Park, J.; Pardo, J.M.; Yun, D.-J. Non-Expresser of PR-Genes 1 Positively Regulates Abscisic Acid Signaling in *Arabidopsis thaliana*. *Plants* **2022**, *11*, 815. [CrossRef]
91. Rasul, F.; Gupta, S.; Olas, J.J.; Gechev, T.; Sujeeth, N.; Mueller-Roeber, B. Priming with a Seaweed Extract Strongly Improves Drought Tolerance in Arabidopsis. *Int. J. Mol. Sci.* **2021**, *22*, 1469. [CrossRef]

92. Denekamp, M.; Smeekens, S.C. Integration of wounding and osmotic stress signals determines the expression of the *AtMYB102* transcription factor gene. *Plant Physiol.* **2003**, *132*, 1415–1423. [CrossRef] [PubMed]
93. Chen, W.-H.; Li, P.-F.; Chen, M.-K.; Lee, Y.-I.; Yang, C.-H. FOREVER YOUNG FLOWER Negatively Regulates Ethylene Response DNA-Binding Factors by Activating an Ethylene-Responsive Factor to Control Arabidopsis Floral Organ Senescence and Abscission. *Plant Physiol.* **2015**, *168*, 1666–1683. [CrossRef] [PubMed]